Vegetation and climate dynamics in the south-western mediterranean during MIS 37–31 (~1.25 - ~1. 06 Ma): Insights from the marine core ODP site 976

Maé Catrain, Nathalie Combourieu-Nebout, Vincent Lebreton, Séverine Fauquette, Odile Peyron, Morgane Fries, Patricia Richard, Lionel Dubost, Sébastien Joannin, Jean-Pierre Suc, et al.

Quaternary Science Reviews 369 (2025) 109635

Contents lists available at ScienceDirect

Quaternary Science Reviews

journal homepage: www.elsevier.com/locate/quascirev

Vegetation and climate dynamics in the south-western mediterranean during MIS 37–31 (~1.25 - ~1. 06 Ma): Insights from the marine core ODP site 976

Maé Catrain [a,*], Nathalie Combourieu-Nebout [a], Vincent Lebreton [a], Séverine Fauquette [b], Odile Peyron [b], Morgane Fries [c], Patricia Richard [c], Lionel Dubost [a], Sébastien Joannin [b], Jean-Pierre Suc [d], Emin Paquier Comas [a,c], Jeanne Lepelletier [a], Marie-Hélène Moncel [a]

[a] HNHP – Histoire Naturelle des Humanités Préhistoriques, UMR 7194 CNRS-MNHN-UPVD, Muséum National D'Histoire Naturelle, Institut de Paléontologie Humaine, Paris, France
[b] ISEM - Institut des Sciences de L'Évolution de Montpellier, UMR 5554 CNRS, Université de Montpellier, Montpellier, France
[c] LSCE - Laboratoire des Sciences Du Climat et de L'Environnement, UMR 8212, CEA-CNRS-UVSQ-IPSL, Université Paris-Saclay, Gif-sur-Yvette, France
[d] Sorbonne Université, CY Cergy Paris Université, CNRS, Institut des Sciences de La Terre de Paris, ISTeP, F-75005, Paris, France

ARTICLE INFO

Handling Editor: Dr Yan Zhao

Keywords:
Late early pleistocene
Vegetation
Pollen
Relict taxa
Glacial and interglacial oscillation
Mediterranean

ABSTRACT

The Early to Middle Pleistocene Transition (EMPT; 1.4 to 0.4 Ma) represents a major change in the Earth's climate, marked by a shift from obliquity-driven glacial cycles of 41,000 years to dominant cycles of 100,000 years. This period is crucial for understanding climate and vegetation change, as it marks the final phase of the disappearance of megatherm and mesotherm forest taxa that had been present in Europe since the Miocene and Pliocene period. However, sedimentary records from this period are sparse, particularly in the Mediterranean region. Here, we present continuous pollen and isotopic records spanning Marine Isotope Stages (MIS) 37–31 (~1.25–1.06 Ma) from site ODP 976 in the Alboran Sea, the first continuous sequence in the Western Mediterranean for this period, which is discussed in light of a corpus of records to reflect the broader dynamics of the Mediterranean vegetation. Pollen data show similar successions around the Mediterranean: steppe vegetation during glacial periods, temperate forests during interglacial periods, and the development of conifers during transition phases, reflecting the gradual shift from 41 ka to 100 ka cycles. Differences in the vegetation composition between the west and the rest of the Mediterranean during Interglacial-Glacial/Glacial-Interglacial transitions are highlighted by the important role of Cupressaceae and Ericaceae. It clearly indicates the scarcity of relict taxa (*Sciadopitys, Cathaya, Eucommia*) south of 40°N, revealing a north-south gradient of decline associated with increasing aridity and challenging the traditional view of "southern refugia."

1. Introduction

The Quaternary period is characterized by alternating warm interglacial phases and cold glacial phases, collectively forming climatic cycles with varying periodicities linked to orbital parameters. During this period, which lasted for 2.6 Ma, the duration of climatic cycles changed, with, notably, the lengthening from 41 kyr, controlled by obliquity, to 100 kyr cycles, linked to eccentricity forcing (Ruddiman et al., 1986; Head and Gibbard, 2015). The period characterized by the transition from a 41 kyr obliquity-driven glacial cycle to a dominant 100 kyr cycle is known as the Mid-Pleistocene Transition (MPT), occurring from around 1.25 to 0.75 Ma (Clark et al., 2006) or, more broadly, as the Early Middle Pleistocene Transition (EMPT), from 1.4 to 0.4 Ma (Head and Gibbard, 2015). This key time period is marked by an increase in global ice volume and a cooling of sea surface temperatures (SST) due to increasingly intense glacial periods (Head and Gibbard, 2015; Herbert, 2023).

These climate changes may have had an impact on the earliest hominin settlement of Western Europe, currently dated to 1.4–1.2 Ma (Carbonell et al., 2008; Huguet et al., 2025; Moyano et al., 2011). Over

* Corresponding author.
E-mail address: mae.catrain@edu.mnhn.fr (M. Catrain).

https://doi.org/10.1016/j.quascirev.2025.109635
Received 4 June 2025; Received in revised form 15 September 2025; Accepted 22 September 2025
Available online 29 September 2025

the past decades, this period has been extensively studied, in particular to determine whether climatic conditions, and thus vegetation and fauna, influenced the early peopling of Western Eurasia (Saarinen et al., 2021; Ochando et al., 2022; Margari et al., 2023). The early phase of the EMPT, approximately spanning Marine Isotope Stages (MIS) 37 to 31 (~1.25 - ~1. 06 Ma) are of particular interest as they were punctuated by two pronounced glacial periods (MIS 34 and 36) and a super interglacial (MIS 31) (Sánchez Goñi et al., 2016; Margari et al., 2023). In addition, during this period, the interglacial periods began to last for longer, in particular, MIS 35 (~45-50ka) (Barker et al., 2022).

During the Miocene (23.03–5.33 Ma), the northern Mediterranean vegetation mainly consisted of subtropical forest and gradually transformed into Mediterranean sclerophyllous vegetation (Suc et al., 2018). From the Pliocene to the Middle Pleistocene, the subtropical vegetation, dominated by *Taxodium, Cathaya, Sequoia,* was progressively replaced by more temperate vegetation, dominated by deciduous *Quercus* and *Carpinus*. The diversity of the forest decreased during this period (Donders et al., 2021). These changes in vegetation are linked to marked climate changes, successive cooling periods: in the middle Miocene (~13.6 Ma), during Early-Late Pliocene transition (~3.6 Ma), the Pliocene-Pleistocene transition (~2.6 Ma) and the Gelasian-Calabrian transition (Suc et al., 2018; Magri et al., 2017). Moreover the increase in the intensity of seasonal drought and the decrease in available moisture, resulting in more widespread steppe plants such as *Artemisia* (Suc and Zagwijn, 1983; Suc, 1984; Combourieu Nebout, 1993; Bertini, 2003; Magri et al., 2017; Suc et al., 2018). The EMPT is a key period for understanding changes in vegetation around the Mediterranean basin and the disappearance of subtropical taxa. The first reconstruction of Eurasian vegetation during the EMPT began in the 1960s–1980s (Ricciardi, 1965; Zagwijn, 1974; Suc, 1984; Suc and Zagwijn, 1983). Recent studies focus on higher resolution analysis to better understand vegetation changes at a regional scale and the timing of the disappearance of relict taxa (e.g., *Sciadopitys, Cathaya, Eucommia*), in the Mediterranean area (Biltekin et al., 2015; Combourieu-Nebout et al., 2015; Magri et al., 2017; Benítez-Benítez et al., 2018; Andrieu-Ponel et al., 2021; Donders et al., 2021; Bertini and Combourieu-Nebout, 2023). These studies reflect the complexity of defining the chronology and geographic trends of these extinctions. Since the Miocene epoch, there have been disparities in vegetation cover, with southern regions already exhibiting more open environments and sparser forests (Suc et al., 2018). Two distribution gradients are often mentioned in the literature, i.e. N-S and E-W, even if the patterns seem more complex (Combourieu-Nebout et al., 2015; Magri et al., 2017; Benítez-Benítez et al., 2018; Suc et al., 2018).

To date, the EMPT is still poorly documented in the Mediterranean, due to the scarcity of long and continuous sequences panning this period. Few continuous sequences cover the end of the Early Pleistocene, especially the period from ~1.25 to 1.06 Ma, corresponding to MIS 37 to 31. Most of these sequences are terrestrial, with very few outcrop sequences and no other continuous marine cores. Only six continuous sequences are available for the whole Mediterranean area: in Spain, Palominas (Altolaguirre et al., 2019, 2020, 2021) and Bòbila Ordis (Julià Bruguès and Suc, 1980; Leroy, 1988, 2008; Suc and Popescu, 2005); in Italy, Monte san Giorgio (Dubois, 2001) and Montalbano Jonico (Joannin et al., 2008); in the Balkan region, Lake Ohrid (Wagner et al., 2019; Panagiotopoulos et al., 2020; Donders et al., 2021) and in Greece, Tenaghi Philippon (Van Der Wiel and Wijmstra, 1987a, 1987b; Tzedakis et al., 2006; Pross et al., 2015). Two sequences only record part of MIS 37-31: e.g., Madonna della strata (Magri et al., 2010) and Fornaci di ranica (Ravazzi et al., 2005) in Italy are associated with stages MIS 37 or 35 and MIS 31. Other available sites from this period yield imprecise dating: e.g., Saint-Macaire (France; Leroy et al., 1994), Pietrafitta (GeMiNa, 1962; Fusco, 2007; Martinetto et al., 2014), Leonessa (Italy; GeMiNa, 1962; Ricciardi, 1965; Fubelli et al., 2008), Leffe (Italy; Ravazzi and Rossignol Strick, 1994; Ravazzi, 1995; Ravazzi and Rossignol Strick, 1995), Monte Poggiolo (Italy; Lebreton, 2004), Mas Grill (Spain; Geurts, 1977), Cal Guardiola (Spain, Postigo Mijarra et al., 2007) and/or insufficient resolution: Mas Miquel (Spain; Geurts, 1977), Moli Vell (Spain; Geurts, 1977; De Deckkers et al., 1979) and Lake Acigöl (Türkiye; Andrieu-Ponel et al., 2021). Reliable representations of the complex dynamics of vegetation and climate around the Mediterranean basin are thus limited, due to the paucity of continuous, well-dated sequences. Long continuous records are crucial in order to advance our knowledge of the EMPT.

We present new continuous isotopic and pollen data obtained for the period between 1.25 and 1.06 Ma (MIS 37 to 31) at the ODP 976 site located in the Alboran Sea. These data complement previous studies carried out on the same core for MIS 31–23 (1.08–0.9 Ma) (Joannin et al., 2011). This site, located in the extreme southwest of the Mediterranean basin, yielded the first marine data for the region. These data are complemented by the continuous sequences published (Leroy, 1988, 2008; Dubois, 2001; Joannin et al., 2008; Pross et al., 2015; Altolaguirre et al., 2020; Donders et al., 2021) throughout the Mediterranean region to enhance the comprehension of the climatic and environmental contexts at the basin scale and over this time period. This study aims to i) better understand vegetation and climate dynamics at a time when 41 ka cycles began to increase in duration and ii) provide a continuous view of the disappearance of some relict taxa in the Mediterranean at the end of the Early Pleistocene.

2. General setting of ODP 976

2.1. Core location and sedimentation

ODP Leg 161 Site 976 (36°12.30N, 4°18.8′W; Fig. 1) is located in the west part of the Alboran Sea, 110 km from the Strait of Gibraltar, about 150 km north of Morocco and about 60 km south of Spain. The core was drilled inside the western Alboran Gyre at a depth of 1108 m (Comas et al., 1996). The sedimentation is composed of homogeneous nannofossil-rich clays and silt. The ODP 976 reference core corresponds to the combination of three holes, B, C and D, to obtain the best recovery of sediments with a composite depth (mcd) calculated using correlations of the susceptibility records of the three holes (Comas et al., 1996). The upper 362 m of sediment correspond to Late Pliocene and Pleistocene lithostratigraphy, with two sedimentary gaps between 284 and 287 mcd and between 190 and 197 mcd (Comas et al., 1996; Joannin et al., 2011).

2.2. Climate, vegetation and sea circulation

The coast of the Mediterranean basin (Fig. 1) is mostly exposed to a Mediterranean climate (CSa), corresponding to a temperate climate with wet, mild winters and warm and dry summers, according to Köppen's classification (e.g., Granada, Oran, Chefchaouen, Malaga). Some areas (e.g., Almeria) correspond to a cold semi-arid climate (BSk), consisting of a steppe with hot summers and cold winters (Köppen, 1936; Quézel and Médail, 2003; Peel et al., 2007; Sánchez-Laulhé et al., 2021). At present, the mean annual temperature is about 17.7 °C along the coast and 15.3 °C at higher altitudes. In this region, summer drought (precipitation <40 mm) lasts between four and five months. Strong levanter winds blow frequently in the Strait of Gibraltar while strong warm winds from the east are sporadically generated by the northward shift of the Inter-Tropical Convergence Zone (Guerzoni et al., 1997). The Vendavel, a cold wind from the Atlantic Ocean, blows from the west. It is more common in winter, and can cause storms (Shaltout and Omstedt, 2014).

The Mediterranean vegetation is organized into successive belts from the seashore to the mountainous hinterland, mainly limited by the minimum temperature of the coldest month (MTCO) (Quézel, 1979; Rivas-Martínez, 1981; Ozenda, 1994; Quézel and Médail, 2003). Five vegetation belts are listed (Fig. 1): infra-Mediterranean (MTCO >7 °C), thermo-Mediterranean (MTCO >3 °C), meso-Mediterranean (0° < MTCO <3 °C), supra-Mediterranean (−3° < MTCO <0 °C),

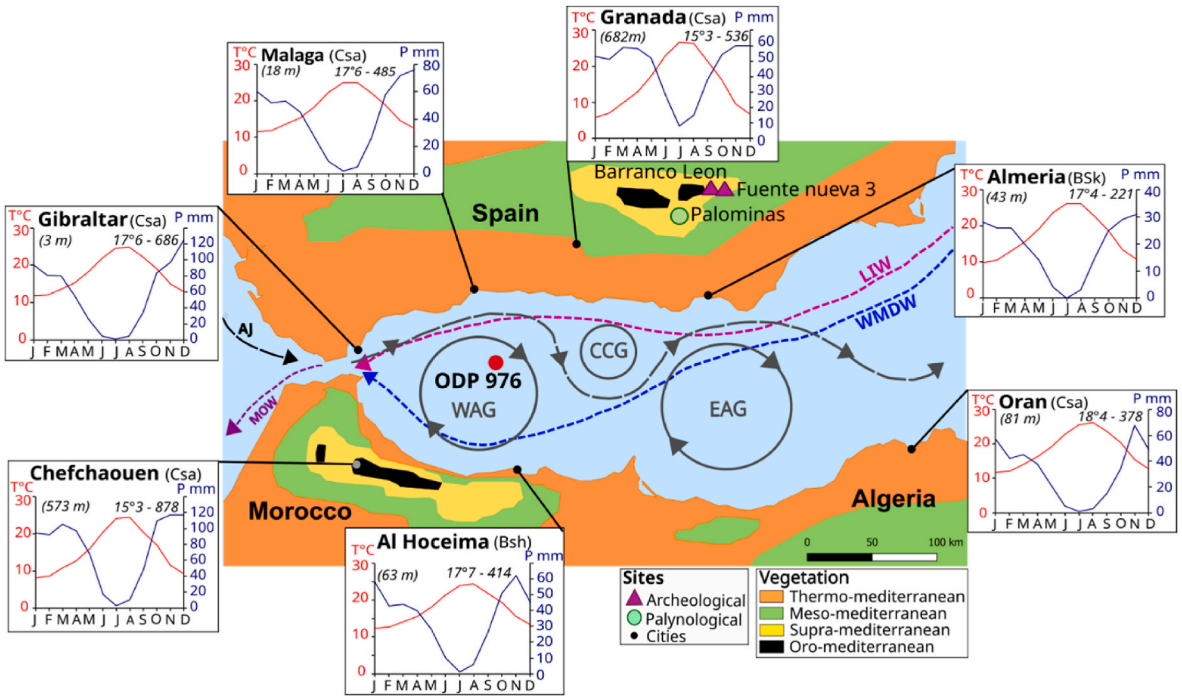

Fig. 1. Location map of the core ODP 976. Ocean circulation in the Alboran Sea (Sánchez-Garrido and Nadal, 2022a; Toti et al., 2020): The Atlantic Jet (AJ), the western Alboran Gyre (WAG), the eastern Alboran Gyre (EAG), the Central Cyclonic Gyre, the Levantine Intermediate Water (LIW), Western Mediterranean Deep Water (WMDW), Mediterranean Outflow Water (MOW). Vegetation and climate in the Alboran Sea edges: ombrothermic diagrams (www.climate-data.org) for several cities around the basin and vegetation belts described by Quézel and Médail (2003). Wind rose of Alboran that represents how many hours a year the wind blows in the direction indicated (www.meteoblue.com).

oro-Mediterranean (−7° < MTCO < −3 °C) (Quézel and Médail, 2003; Médail, 2022). The infra-Mediterranean belt only develops on the southern coast of Morocco and is characterized by *Argania spinosa* and *Acacia gummifera,* with some *Euphorbia*. The thermo-Mediterranean belt (0 m < altitude <300–700 m) is mainly composed of *Olea, Ceratonia, Pistacia, Chamaerops humilis, Juniperus* and *Tetraclinis*. The meso-Mediterranean belt (with an altitude range of 300–700 m to 1000–1200 m) is primarily a forest dominated by *Pinus halepensis* and several evergreen *Quercus* species *(e.g., Q. ilex, Q. coccifera, Q. suber)*. Deciduous oaks, in particular *Quercus pubescens,* as well as *Ostrya carpinifolia* and *Carpinus orientalis*, grow in the supra-Mediterranean forested belt (1000–1200 m < altitude <1500–1700 m). Mediterranean mountain (oro-Mediterranean) belts (1500–1700 m < altitude <2000–2300 m) consist mainly in a conifer forest with *Juniperus, Pinus nigra, Cedrus* (only in Morocco today) and *Abies* (Benabid, 1985; Ozenda, 1994; Quézel and Médail, 2003; Médail, 2022).

Atlantic waters, called the Atlantic jet, enter the Mediterranean Sea through the Strait of Gibraltar (Fig. 1). These waters circulate on the surface from west to east of the Alboran Basin through two main oceanic gyres, the Western Alboran gyre (WAG) and the Eastern Alboran gyre (EAG) and a smaller one, the Central Cyclonic Gyre (CCG) (Sánchez-Garrido and Nadal, 2022b). At depth, the Levantine Intermediate Water (LIW) and the Western Mediterranean Deep Water (WMDW), which are denser and saltier, circulate from east to west. These two currents exit into the Atlantic through the strait and form the Mediterranean Outflow Water (MOW) (Tintore et al., 1988; Fabres et al., 2002; Pérez-Folgado et al., 2003; Moreno et al., 2005; Macias et al., 2016).

3. Materials and methods

3.1. Age model methods

Several age models have been constructed for this core over the EMPT using either MIS correlation of the planktonic foraminiferal $\delta^{18}O$ curve (von Grafenstein et al., 1999), ocean surface temperature reconstructions (González-Donoso et al., 2000), or calibration points, defined notably with calcareous nannofossil events, sapropels and marine isotopic stage transitions (Joannin et al., 2011). In the present work, control points are based on two sapropels (Lourens, 2004; De Kaenel et al., 1999; Murat, 1999), a nannofossil event, the Lower Occurrence of *Reticulofenestra asanoi* (Reale and Monechi, 2005) and the MIS transitions obtained by correlations between the $\delta^{18}O$ ODP 976 record and the $\delta^{18}O$ reference curves of the Mediterranean (Wang et al., 2010), and the global ocean stack from Lisiecki and Raymo (2005) (Fig. 3B). A linear regression was applied from these fixpoints. As the resolution of the $\delta^{18}O$ isotope curve of the ODP 976 from von Grafenstein et al. (1999) was not sufficient (25 samples, with one sample every metre), new stable isotope measurements were carried out here to detect the position of the MIS transitions more precisely.

3.2. Stable isotope analysis

Stable oxygen isotopes were measured in fifty-six samples (spacing 7 cm–100 cm, an average of every 30 cm) of shallow deep-living planktonic foraminifera *Globigerina bulloides* (range 250–315 μm). Between eight to twelve individuals were selected. Methanol and ultrasound were used to clean the tests without altering them. Analyses were performed at the Laboratory for Sciences of Climate and Environment (LSCE, France with analytical platform PANOPLY) on an Isoprime dual-inlet Isotope Ratio Mass Spectrometer (Elementar). The measurements of $\delta^{18}O$ values (expressed in ‰) are reported versus the Vienna Pee Dee Belemnite standard (VPDB) with respect to 603 ($\delta^{18}O$ = -2.37 ‰) and NBS 18 ($\delta^{18}O$ = -23.2 ‰) standards.

3.3. Pollen analysis

One hundred and twenty-two pollen samples were collected between

258.72 and 281.23 mcd (metre composite depth) with a spacing of 2 cm–40 cm (average every 18 cm). Samples were processed using a standard method derived from Combourieu Nebout et al. (1999) and Sassoon et al. (2023). Foraminifera were first separated by sieving at 150 μm, then HCl (33 %) and HF (70 %) attacks were performed to extract the pollen grains, followed by ultrasound and 10 μm sieving. Two aliquot tablets of *Lycopodium* were added at the beginning of the pollen process to calculate palynomorph concentrations. A minimum of 150 grains (more than 300 grains including *Pinus*) and a minimum of 15 taxa were counted for each sample. The Main Pollen Sum (MPS) sum excluded aquatics (e.g., *Typha, Sparganium*) and Pteridophyte spores (e.g., *Isoetes, Pteris*), as well as *Pinus* due to its overrepresentation in the marine record (Heusser, 1988; Fletcher and Sánchez Goñi, 2008; Beaudouin et al., 2007; Joannin et al., 2011). Pollen grains were identified using reference slides and iconographic atlases (e.g., Beug, 2004; Reille, 1992). The three samples at the top of our pollen sequence were analysed by Joannin et al. (2011). The microflora is composed of 144 taxa classified into different ecological groups (Table 1). Pollen percentages were calculated using MPS sum except for *Pinus*, aquatic plants and fern spores, which were calculated using the total sum of pollen grains (TSP). Pollen analysis of a marine sequence provides a regional record which will cover the vegetation of southern Spain and northern Morocco in the case of ODP 976 core. Percentage diagrams were drawn using TILIA software (version 3.0.1; Grimm, 1991).

Pollen zones were generated using the CONISS (Constrained Incremental Sum of Squares) clustering method available in the Tilia software (version 3.0.1), based on the total number of taxa. The pollen zones were then manually refined based on a visual interpretation of the CONISS results.

4. Results

4.1. Isotopes and age model results

The $\delta^{18}O$ values obtained from the fifty-six new samples were added to the twenty-five $\delta^{18}O$ values previously obtained by von Grafenstein et al. (1999). In this way, we obtained a high-resolution isotope curve to better define the position of the different MIS (Fig. 2). The curve from the study by von Grafenstein et al. (1999) linked the final stage before a sedimentary gap between 284 and 287 mcd to MIS 35. However, complementary analyses have now refined this interpretation. According to the new data, the intense interglacial at the base of the series is now attributed to MIS 37 rather than MIS 35, as MIS 37 is clearly identified as a well-expressed interglacial in both Mediterranean and global reference curves (Lisiecki and Raymo, 2005; Wang et al., 2010). Consequently, the position of the MIS 34–35 transition moved from 276.46 to 269.1 mcd (Fig. 2). The transition between stages 31 and 30 has also been moved from 258.47 to 256.53 mcd (Fig. 2). The more accurate positioning of these MIS helps to define fixpoints based on the association of our depths with the transition dates of the transition defined by Lisiecki and Raymo (2005).

The new age model (Fig. 3A) follows a linear regression based on 10 fixpoints (Fig. 3B): seven MIS transitions, sapropel 625 dated around 1144 ka, sapropel 624 dated around 1111 ka (Lourens, 2004; De Kaenel et al., 1999; Murat, 1999), and the Lower Occurrence of *Reticulofenestra asanoi,* corresponding to the MIS 34-33 transition, dated around 1141 ka (Reale and Monechi, 2005).

The time resolution of sampling corresponds to ~350–~4000 years (with an average of 1400 years) for pollen data and ~800–~6000 years (mean ~ 2400 years) for oxygen isotopes. These ages are obtained by interpolation between the fixpoints.

Table 1
Composition of the ecological groups. The asterisk * identifies relict taxa.

Ecological groups	Taxa
Subtropical group	Euphorbiaceae *Croton* type, *Myrica*
Temperate forest	*Acer, Alnus, Betula, Carpinus betulus, Carpinus orientalis/Ostrya* type, *Carya*, Castanea, Corylus, Fagus, Fraxinus, Hedera, Ilex, Jasminum, Juglans, Ligustrum, Platanus, Populus, Pterocarya*, Quercus* deciduous type, *Salix, Tamarix, Ulmus/Zelkova* type*
Montane forest	*Abies, Cathaya*, Cedrus, Picea, Tsuga**
Mediterranean group	Cistaceae, *Cistus, Cistus ladanifer* type, *Myrtus, Nerium oleander, Olea, Pistacia, Phillyrea, Quercus ilex* type, *Rhus*
Open vegetation	*Alyssum* type, *Ambrosia,* Apiaceae, *Armeria, Asphodelus,* Asteraceae Asteroideae, Brassicaceae, *Carduus* type, Caryophyllaceae, *Centaurea, C. cyanus* type, *C. jacea* type, *C. scabiosa* type, Asteraceae Cichorioideae, Convolvulaceae, *Convolvulus,* Crassulaceae, Cyperaceae, *Euphorbia,* Euphorbiaceae, Fabaceae, Gentianaceae, Geraniaceae, *Helianthemum, Knautia,* Lamiaceae, Liliaceae, *Linum,* Malvaceae, *Mercurialis* type, Papaveraceae, *Paronychia/Hernaria* type, *Plantago,* Plumbaginaceae, Poaceae, *Polygonum,* Ranunculaceae, Rosaceae, *Sangisorba, Saxifraga, Scabiosa,* Scrophulariceae, *Silene* type, *Stellaria* type, *Valeriana, Valerianella*
Steppe	Amaranthaceae, *Artemisia, Calligonum, Ephedra distachya, Ephedra fragilis, Erodium, Lygeum*

4.2. Pollen analysis

The pollen sum is between 126 and 268 grains (mean: 183) for the Main Pollen Sum (MPS) and between 223 and 562 (349 grains) for the Total Sum of Pollen (TSP). Only three samples were excluded from the diagram due to their low pollen counts; at the beginning of MIS 32 (at ~1100 and at ~1102 ka) and during MIS 37 (at ~1223 ka). Between 15 and 28 pollen taxa were determined, distributed into 31 families and 72 genera. The pollen assemblages correspond to a typical Mediterranean vegetation organized into altitudinal belts with meso- and thermo-Mediterranean vegetation characterized by *Pinus*, *Quercus deciduous* type, *Q. ilex* type, *Carpinus*, *Cistus*, *Ostrya*, *Olea* and Cupressaceae (*Cupressus/Juniperus* type), and a Mediterranean mountainous vegetation belt dominated by *Cedrus* and *Abies*. The coastal area is characterized by common Mediterranean open vegetation and steppe plants, such as Asteraceae, Poaceae, *Ephedra*, Amaranthaceae and *Artemisia*.

Based on the CONISS clustering method and the variations in percentages of the main taxa, eight pollen zones and eleven pollen subzones were delimited. They correspond to the main phases of changes in vegetation between 1.235 and 1.063 Ma, or to the time-period from the end of MIS 37 to MIS 31 (Fig. 4, Table 2). Vegetation changes consist mainly of fluctuations between deciduous *Quercus* forest and steppic environments (with *Artemisia, Ephedra* and Amaranthaceae), reflecting climate oscillations between warm/humid and cold/dry conditions (Fig. 4, Table 2).

Quercus deciduous-type is the main component of the temperate forest, associated with *Fraxinus* and *Carpinus,* and highlights warm/humid phases (pollen zones: I, III, V, VIII), as well as the development of fern and aquatic plants; cf *Isoetes*. From MIS 33 onwards (~1.114 Ma), the temperate forest appears to be more diversified with the presence of *Carpinus betulus, Carpinus orientalis/Ostrya* type, *Corylus, Fraxinus, Salix* in pollen zones V, VI, VII, VIII. The maximum diversity is observed during MIS 31 (1.081–1.062 Ma), with the occurrence of *Pterocarya, Juglans* and *Ulmus/Zelkova*-type in pollen zones VIII.a, VIII.b. A few relict taxa occur sporadically in the temperate forest component, such as *Carya* (pollen zone IV.a) and *Pterocarya* (pollen zones VII, VIII.a, VIII.b), while in the montane forest, *Cathaya* (pollen zone I.a) and *Tsuga* (pollen zone I.b, VII) are occasionally present. The pollen assemblage only shows occurrences of relict taxa. The development of an Ericaceae phase at the end of each interglacial period probably indicates cooler and wetter conditions.

Repetitive increases of *Artemisia*, Amaranthaceae, *Ephedra* indicate the development of steppe phases. At the same time, Cupressaceae and high-altitude conifer forest taxa develop, particularly *Cedrus*, then *Abies* and *Picea,* mainly in the nearby mountains (pollen zones II.a, II.b, IV.b, IV.c, VI, VII).

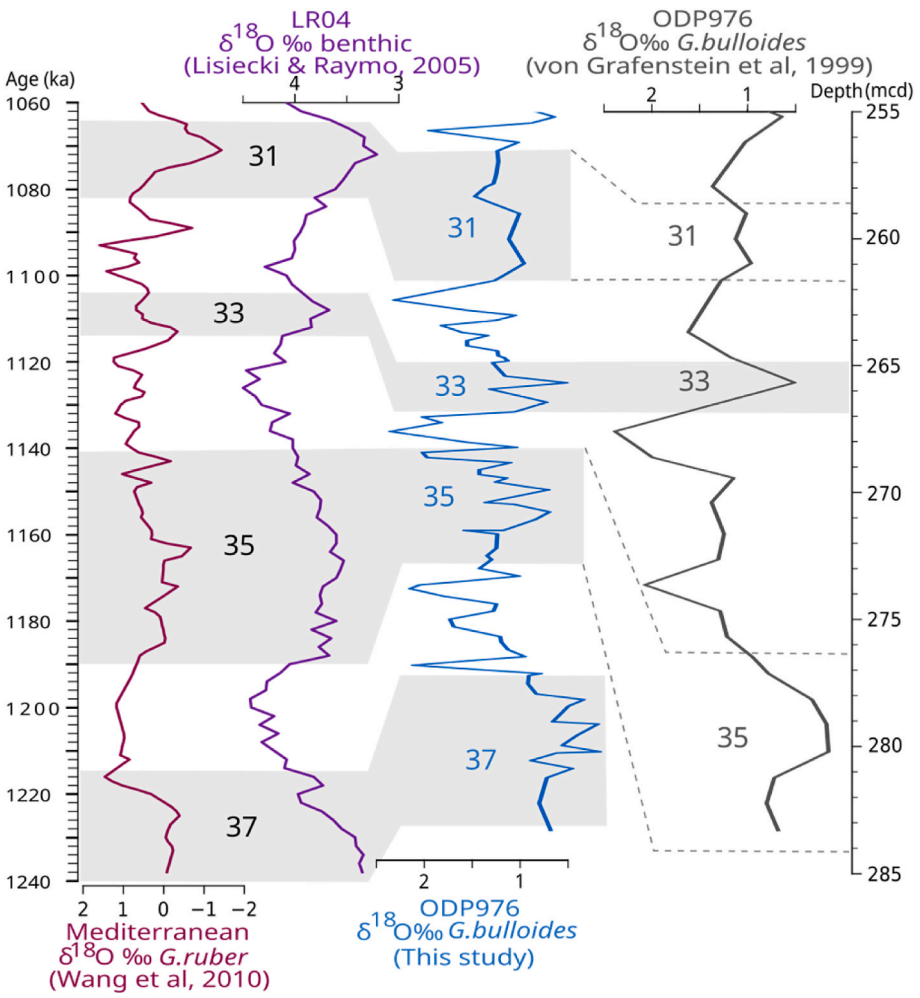

Fig. 2. Correlation between Mediterranean (magenta), Global (purple) and ODP 976 $\delta^{18}O$ isotopes curves (blue and grey curves). The grey line corresponds to the isotope curve by von Grafenstein et al. (1999) and the blue curve shows all the isotopic data, including our new measurements. ODP 976 curves are plotted against to depth. The grey dotted lines represent the previous MIS 35 correlation by von Grafenstein et al. (1999) and the grey bars shows the updated correlation.

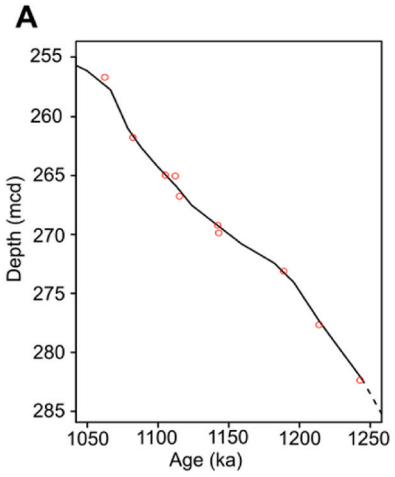

B

Type	Name	Depth (mcd)	Age (ka)
MIS transition	31-30	256.53	1062
MIS transition	32-31	261.64	1081
MIS transition	33-32	264.84	1104
Sapropel	624 (i-104)	264.913	1111
Nanofossil	LO *Reticulofenestra asanoi* (MIS 34-33)	266.63	1114
MIS transition	35-34	269.1	1141
Sapropel	625 (i-108)	269.745	1144
MIS transition	36-35	272.99	1190
MIS transition	37-36	277.54	1215
MIS transition	38-37	282.24	1244

Fig. 3. Age-depth model of ODP 976 between 255 and 285 mcd. A: Age model curve with the fixpoints used (red circles). B: Table of fixpoints. LO: Lowest Occurrence.

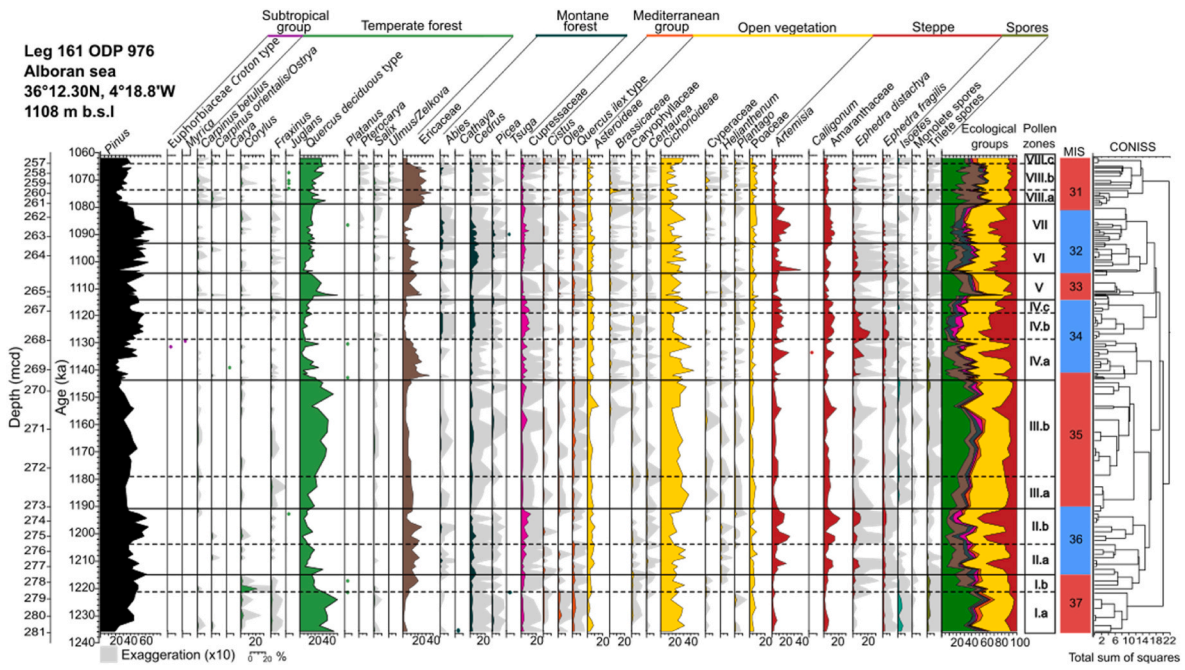

Fig. 4. ODP 976 summarized pollen diagram according to depth and age. Ecological groups (see Table 1 for composition details), pollen zones with CONISS clustering and the MIS chronology with glacials in red and interglacials in blue. Here, Cupressaceae is the *Cupressus/Juniperus* type. The percentages of *Pinus* and spores are calculated in the total counted pollen grains and percentages of the other taxa are calculated excluding pine, spores, aquatic and indeterminate palynomorphs.

5. Discussion

5.1. Mediterranean vegetation changes during the late Early Pleistocene

5.1.1. Vegetation succession recorded in the Alboran Sea

The ODP 976 vegetation oscillations are clearly correlated with the planktonic $\delta^{18}O$ variations from the same core and are consistent with the $\delta^{18}O$ variations in the global record (LR04; Fig. 5; Lisiecki and Raymo, 2005).

The high-resolution pollen record on ODP 976 shows alternating temperate and steppic vegetation phases between MIS 37 and 31, each illustrating successive vegetation shifts. All along our pollen record, the general pattern shows five distinct phases, starting with a cold/warm transition period (Figs. 5 and 7):

1) Development of Cupressaceae indicating the onset of wetter conditions.
2) Expansion of temperate deciduous forest linked to warmer and wetter conditions. Mainly dominated by *Quercus* deciduous type, *Fraxinus*, *Carpinus* and *Corylus*, the forest also includes some Mediterranean taxa, such as *Quercus ilex* type and *Cistus*. Forest development coincides with interglacial periods.
3) Development of Ericaceae indicating cooling and persistence of wet conditions throughout the year due to a reduction of evaporation and seasonality.
4) Expansion of the high-altitude conifer forest (particularly *Cedrus*) showing a return to cool-humid conditions and indicating the transition from an interglacial to a glacial period.
5) Expansion of steppe taxa (*Artemisia,* Amaranthaceae*, Ephedra distachya* and *E. fragilis*) indicating the onset of drier/colder conditions, typically observed during glacial episodes.

These successions were also observed between MIS 30 and 23 (1060–900 ka) in the ODP Site 976 (Joannin et al., 2011), showing similar vegetation dynamics at the end of the Early Pleistocene.

5.1.2. An overview of late Early Pleistocene mediterranean vegetation around the Mediterranean Sea

Six late Early Pleistocene continuous long sequences are contemporaneous with ODP 976: Palominas in southern Spain (Altolaguirre et al., 2019, 2020, 2021), Bòbila Ordis in northern Spain (Julià Bruguès and Suc, 1980; Leroy, 1988, 2008; Suc and Popescu, 2005), Monte San Giorgio (Dubois, 2001) and Montalbano Jonico in southern Italy (Joannin et al., 2008), Lake Ohrid (Wagner et al., 2019; Panagiotopoulos et al., 2020; Donders et al., 2021) and Tenaghi Philippon (Van Der Wiel and Wijmstra, 1987a, 1987b; Tzedakis et al., 2006; Pross et al., 2015) in the Balkans and Greece, respectively (Fig. 6). Similar interglacial and glacial cycles are depicted by fluctuations in temperate forest and steppe taxa across Montalbano Jonico, Lake Ohrid, Tenaghi Philippon and ODP 976. Bòbila Ordis, Palominas and Monte San Giorgio show different patterns. In Bòbila Ordis, glacial periods are represented by open vegetation. In Palominas, the local vegetation includes *Pinus,* highlighting glacial-interglacial variations. In Monte San Giorgio, *Pinus* and temperate taxa represent fluctuating warm and cold periods.

Ericaceae are more abundant in the ODP 976 record, reaching up to 30 %, compared to the other sites (Fig. 6). Based on current vegetation distribution in southern Spain and northern Morocco, the Ericaceae recorded in our data probably include *Arbutus, Arctostaphylos, Erica, Rhododendron ponticum* and *Vaccinium uliginosum* (Castroviejo et al., 1993). Similar proportions have been found in more recent time periods (MIS 20 to 19 and MIS 30 to 23), and interpreted as a response to increasing oceanic influences (Joannin et al., 2011; Toti et al., 2020). This is also supported by the high percentages of Ericaceae recorded in the marine core U1385 off Portugal during MIS 19 (Sánchez Goñi et al., 2016).

Mediterranean taxa are poorly or not at all represented at the Mediterranean sites, except in Palominas (Fig. 6). This high proportion of Mediterranean taxa in southern Spain is corroborated by significant percentages of *Quercus ilex* type and *Olea* recorded in the nearby contemporaneous archaeological sites of Fuente Nueva 3 and Barranco Leon (Ochando et al., 2022). Such vegetation is typical of thermo- and meso-Mediterranean vegetation belts and represents the local

Table 2
Description of pollen zones.

Zones	Depth (mcd)	Age (ka BP)	Pollen description
VIII.c	256.53–257.29	1062–1064.83	*Quercus deciduous* type constant (20 %). Low percentage of Ericaceae (~5 %). Increase of Mediterranean taxa (~6 %) and Cichorioideae (~30 %). *Ephedra distachya* is absent.
VIII.b	257.29–259.50	1064.83–1073.04	Low percentages of *Quercus deciduous* type (~18 %) and Ericaceae constant around 26 %. Presence of *Corylus*, *Juglans* and *Ulmus/Zelkova*. Continuous herbaceous taxa with a peak of Asteraceae Cichorioideae (23 %) and an increase of Cyperaceae (~5 %). Steppic taxa (~13 %) and *Cedrus* (~2 %). Cupressaceae decrease (2-0 %) and Mediterranean taxa are absent.
VIII.a	259.50–261.12	1073.04–1079.07	*Quercus* deciduous type (up to ~20 %), *Carpinus betulus* (~1 %), *Carpinus orientalis/Ostrya* (~0.8 %), *Fraxinus* (~0.8 %), *Pterocarya* (~0.2 %) and *Salix* (~0.6 %). Ericaceae up to (21–37 %). Herbaceous taxa, Cupressaceae and *Quercus ilex* type with continuous record. Brassicaceae and Caryophyllaceae increase (16 %). *Artemisia* down to 3 % and Amaranthaceae down to 2.5 %. *Ephedra fragilis* and *Ephedra distachya* absent. *Picea* only present at the beginning and *Cedrus* rising at the end. Fern spores.
VII	261.12–263.41	1079.07–1093.72	High percentages of *Artemisia* (up to 24 %), Amaranthaceae (up to 15 %). *Ephedra* decrease. *Quercus* deciduous type, herbaceous plant (Asteraceae Cichorioideae: ~17 %, Asteraceae Asteroideae: ~6 %, Poaceae: ~6 %) and Cupressaceae (~4 %) in constant values. Low percentages of Ericaceae. Maximum percentages in montane taxa (*Cedrus* ~11.5 %. *Abies* ~5.5 % and *Picea* ~5 %). *Tsuga* and *Platanus* only in one sample. Ferns absent.
VI	263.41–264.85	1093.72–1104.95	*Quercus* deciduous type decrease (down to ~4 %). Herbaceous (~34.5 %) and Ericaceae (~12 %) decrease slightly. Steppic taxa decline (44–12 %) with a high peak of *Artemisia* (38 %) at 1102.79 ka. Increase in montane elements: *Cedrus* (3–12 %), *Abies* (0.3–3.7 %) and *Picea* (0.6–3.2 %). Cupressaceae rise (0.6–5.5 %).
V	264.85–266.72	1104.95–1114.98	*Quercus* deciduous type high percentages (49.3 % around 1112 ka). Low values of *Carpinus betulus*, *Fraxinus* and *Corylus*. Montane taxa and Cupressaceae decrease. Ericaceae increase. *Quercus ilex* type slightly increase up to 3 %. *Artemisia* and Amaranthaceae respectively up to 5.5 %. and 1.5 %. *Ephedra distachya* and *Ephedra fragilis* at the end respectively up to 9 and 5 %.
IV.c	266.72–267.12	1114.98–1119.35	*Quercus* deciduous type and Ericaceae remain low. *Abies* disappear and *Cedrus* is constant. *Ephedra distachya* decrease (13–3 %). Cupressaceae start to decrease. Herbaceous taxa stable except Asteraceae Cichorioideae, which increase sharply up to 37 %.
IV.b	267.12–267.92	1119.35–1128.10	Low percentages of *Quercus* deciduous type (6 %) and Ericaceae (2.5 %). Cupressaceae (up to 12 %) and altitudinal taxa expand, particularly *Cedrus* (up to 7 %) and *Abies* (4 %). Steppic plants with high values: *Artemisia* (~9 %), Amaranthaceae (~11 %), and *Ephedra* (~18 %). Mediterranean taxa and ferns absent.
IV.a	267.92–269.59	1128.10–1143.27	Some sub-tropical taxa. *Myrica* and Euphorbiaceae *Croton* type. Decrease in *Quercus* deciduous type. *Platanus* and *Carya*. Well-developed Ericaceae heathland. Sporadic Mediterranean taxa (*Cistus, Quercus ilex* type). Two events where the ratio between herbaceous and steppic plants is modified are recorded at around 1133 and 1141 ka. Presence of *Calligonum*. Decrease in ferns.
III.b	269.59–272.19	1143.27–1178.66	*Quercus* deciduous type up to 43 % and heathland down to 3 %. Steady percentages of *Cedrus* and increase in *Picea*. Cupressaceae abundant at around 1158 and 1145 ka. Peak of steppic plants at around 1154 ka with 12 % of *Artemisia* and 17 % of Amaranthaceae. Brassicaceae present around 1164 ka. *Quercus ilex* type increase. Presence of trilete spores and *Isoetes*.
III.a	272.19–273.29	1178.66–1191.65	*Quercus* deciduous type and *Fraxinus* increase to 21 and 2 %, respectively. Steppic and Cupressaceae formations decrease. *Cedrus* and *Isoetes* increase to 2 and 1 %, respectively.
II.b	273.29–275.59	1191.65–1204.28	*Quercus* deciduous type down to 2 %. *Juglans* present. Ericaceae decrease from 25 to 4 %. Montane taxa decrease and ferns are absent. Increase of steppic taxa around 1200 ka and 1193 ka: *Artemisia* (23.6 % and 16.6 %), Amaranthaceae (14 % and 21.5 %), and *Ephedra distachya* (5.6 and 10.8 %).
II.a	275.59–277.54	1204.28–1215	*Quercus* deciduous type and ferns respectively down to 9 and 0 %. Increase in herbaceous taxa with *Poaceae* (10 %), Asteraceae Asteroideae (9 %) and Asteraceae Cichorioideae (33 %). Increase in *Abies*. Steppic plants increase, with a maximum around 1210 ka.
I.b	277.54–278.63	1215–1221.72	*Quercus* deciduous type down to 15 %. *Corylus* peaks (21 %) at 1220 ka. Herbaceous taxa rise to 48 % with: Asteraceae Cichorioideae (~32 %), Asteraceae Asteroideae (~6 %), Poaceae (6 %), and Caryophyllaceae (~2.7 %). Ericaceae present. *Cedrus* and

(*continued on next page*)

Table 2 (*continued*)

Zones	Depth (mcd)	Age (ka BP)	Pollen description
I.a	278.63–280.92	1221.72–1235.85	Cupressaceae up to 14, 8 and 3 %, respectively. Fern spores decrease. Low percentages of Ericaceae (<5 %). Cupressaceae (<3 %). *Cedrus* (~3 %) and *Picea* (~1 %). *Isoetes* and trilete spores are present. Mediterranean taxa up to 6.5 %. Presence of *Platanus*. *Cathaya* and *Tsuga*.

vegetation. On the contrary, the sparsity of Mediterranean taxa in the ODP 976 record may express the regional signal of Alboran Sea borderlands recorded in a marine core that embraces all the altitudinal belts. The pollen composition of the assemblages is clearly influenced by their position in the basin and/or their altitude.

Such vegetation shifts have already been evidenced in the Mediterranean region during the Early and Middle Pleistocene (Combourieu-Nebout, 1993; Popescu et al., 2010; Leroy, 2007; Leroy et al., 2011; Bertini and Combourieu-Nebout, 2023). Two theoretical patterns were previously constructed to represent the vegetational succession during Early Quaternary climate cycles (Fig. 7e f). Combourieu-Nebout et al. (2015) proposed a theoretical model of Early Pleistocene (Gelasian-Calabrian Transition at 1.8 Ma) vegetation dynamics based on the Crotone pollen sequence from southern Italy. This model identified a cyclical pattern in vegetation development, characterized by a transition from open steppe environments during glacial periods to subtropical forests during interglacial peaks. Between interglacials and glacials, transition phases were expressed by temperate deciduous forests (beginning of interglacials) and high-altitude coniferous forests (end of interglacials) (Fig. 7f; Combourieu-Nebout, 1993; Bertini and Combourieu-Nebout, 2023). In Europe, Leroy (2007) and Leroy et al. (2011) defined a slightly different pattern for the Early Pleistocene (based on several sites such as Bòbila Ordis; Fig. 7e), with glacial steppes replaced by open environments, then mixed and deciduous temperate forests during interglacial optima. The interglacial downward transition phase is marked by the expansion of coniferous forests. Three other patterns can be proposed to describe vegetational succession during the MIS 37 to 31 period. At Montalbano Jonico (Italy), variations between interglacial and glacial phases are also described by temperate and steppic vegetation, this time complemented by open vegetation (Fig. 7b). The transition between cold and warm periods comprises Cupressaceae, and at the end of this transition phase, the onset of temperate forest development. The second transition from warm/humid to cold/dry conditions corresponds to high-altitude forest. At Lake Ohrid (Albania), the general pattern of glacial-interglacial cycles shows a transition from open/steppe environments to deciduous forests, with transitional phases marked by the development of high-altitude coniferous forests (Fig. 7c; Panagiotopoulos et al., 2020; Donders et al., 2021). The vegetation at Tenaghi Philippon (Greece) is dominated by open herbaceous formations during the whole period (MIS 37 to 31). Nevertheless, three phases can be identified: a steppic vegetation phase during the glacial periods and a deciduous temperate forest phase during interglacial periods, with in between, at the end of interglacials, a short transition phase with a high-altitude coniferous forest (Fig. 7 d; Pross et al., 2015). This model had already been identified in the Gulf of Corinth for the Early and Middle Pleistocene (Rohais et al., 2007). No patterns representing vegetation successions could be produced at Palominas and Monte San Giorgio as interglacial and glacial phases were poorly defined by pollen and/or uncertainties linked to the definition of MIS. Vegetation successions could be envisaged at Palominas, but this would entail redefining the MIS stages, probably up to stage 33, rather than 34.

All these Mediterranean records show a similar pattern around glacial minima and interglacial maxima. Steppe-like environments are typical of cold, dry glacial periods while interglacial periods are marked

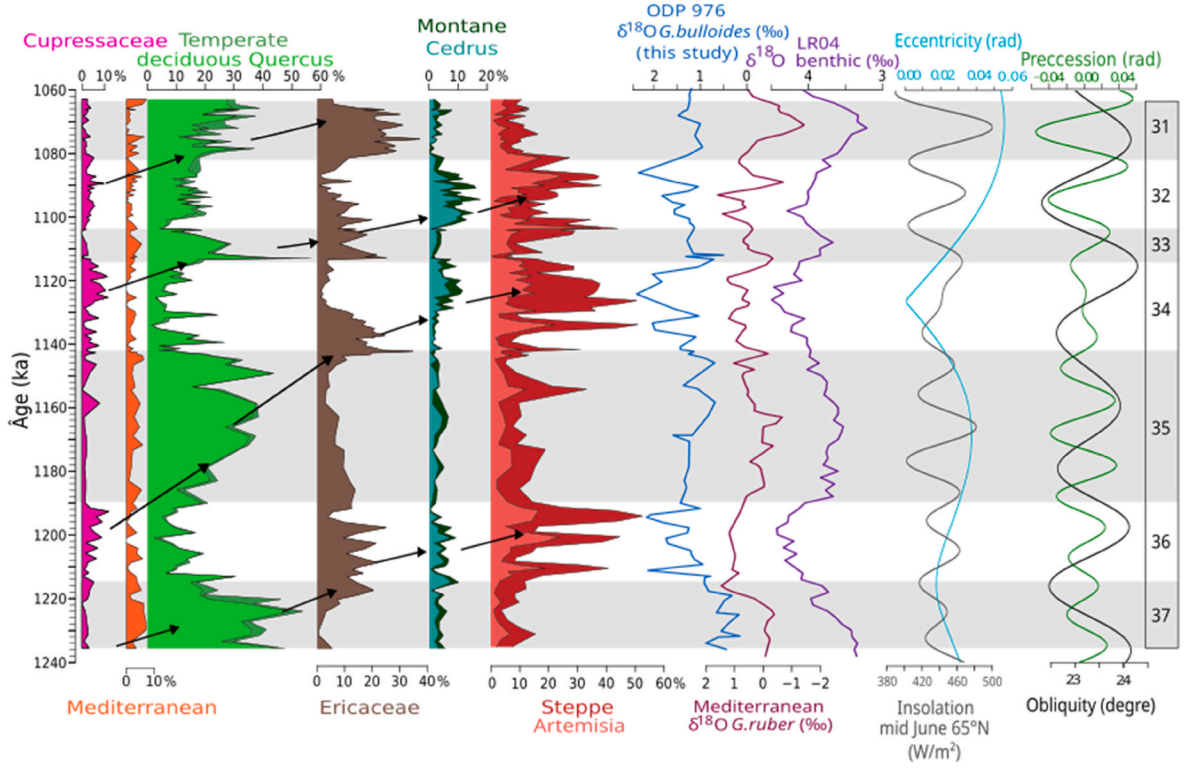

Fig. 5. Cyclic vegetation changes between MIS 37 and MIS 31 recorded in pollen data from ODP 976. $\delta^{18}O$ isotope curves from ODP Site 976 (this study), Mediterranean stack (Wang et al., 2010) andLR04 (Lisiecki and Raymo, 2005), Orbital parameters: eccentricity, obliquity (Laskar et al., 2004), precession and summer insolation at 65°N (Berger and Loutre, 1991) are also plotted.

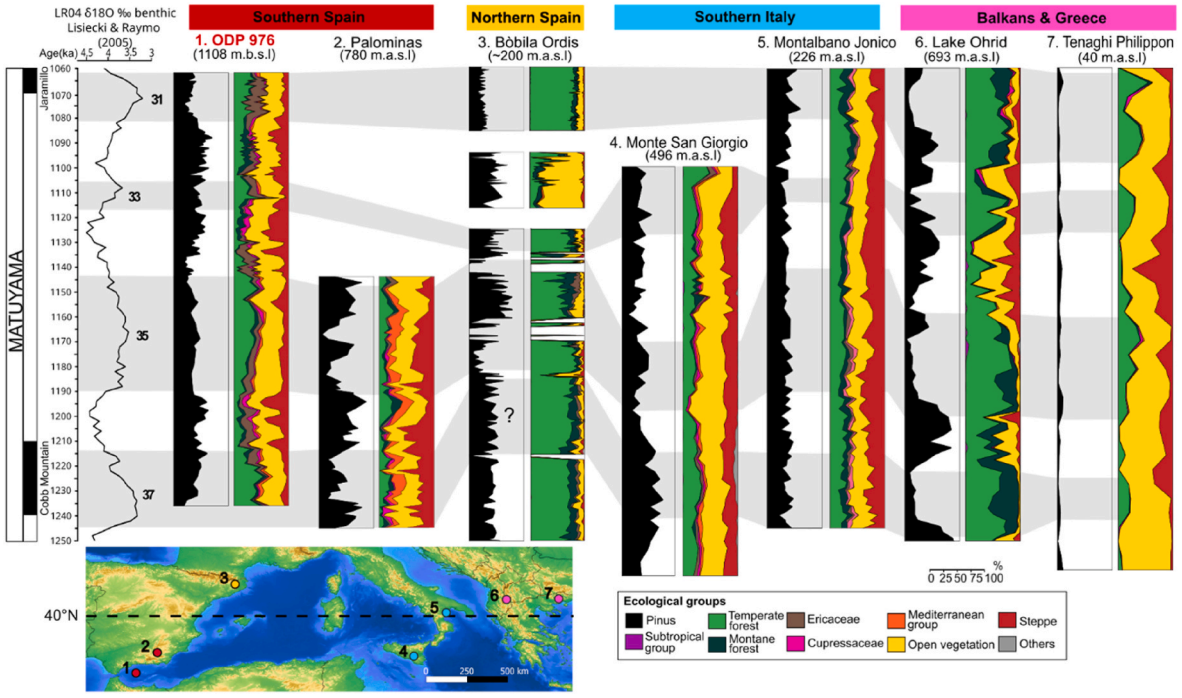

Fig. 6. Pollen-based ecological groups inferred from palynological sequences covering the same time interval as our study on ODP 976 (MIS 37 to MIS 31). Records: 1. ODP 976 (this study), 2. Palominas (Altolaguirre et al., 2019, 2020, 2021), 3. Bòbila Ordis (Julià Bruguès and Suc, 1980; Leroy, 1988, 2008; Suc and Popescu, 2005), 4. Monte San Giorgio (Dubois, 2001), 5. Montalbano Jonico (Joannin et al., 2011), 6. Ohrid Lake (Wagner et al., 2019; Panagiotopoulos et al., 2020; Donders et al., 2021) 7. Tenaghi Philippon (Van Der Wiel and Wijmstra, 1987a, 1987b; Tzedakis et al., 2006; Pross et al., 2015). We used the same ecological groups for each site (see Table 1). OPD 976 and Montalbano Jonico are plotted according to age, other sites are plotted according to depth. The shaded interval marked with "?" highlights an uncertain attribution of the MIS for the Bòbila Ordis sequence.

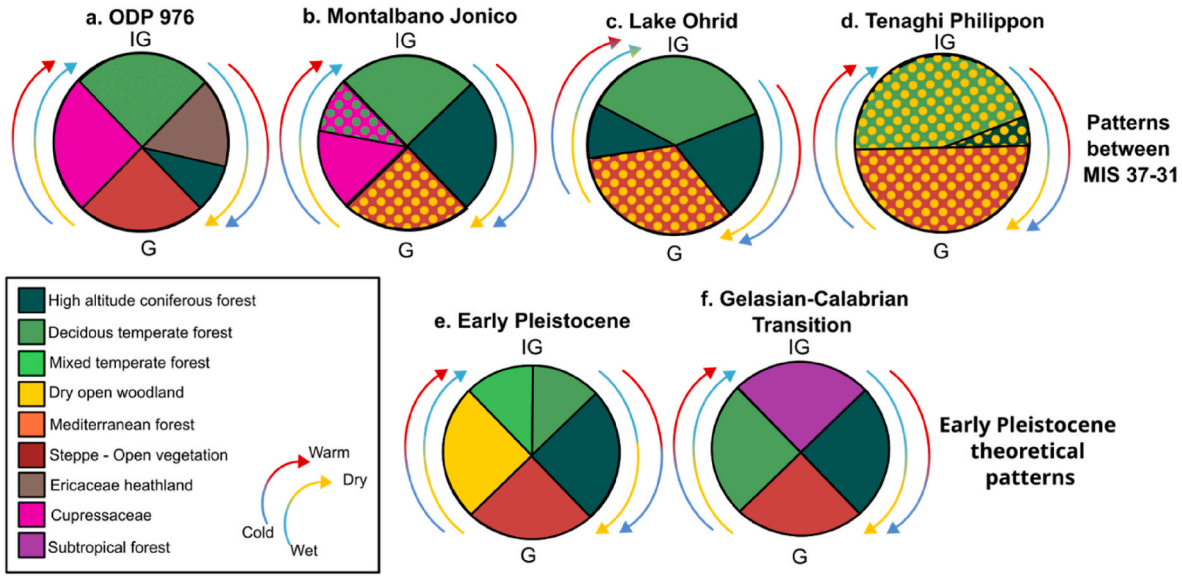

Fig. 7. Different models proposed for vegetation cycles during the Early and Middle Pleistocene. From left to right: a. ODP 976 (this study), b. Montalbano Jonico (Joannin et al., 2008), c. Lake Ohrid (Panagiotopoulos et al., 2020; Donders et al., 2021), d. Tenaghi Phillippon (Pross et al., 2015), e. The Early Pleistocene in Europe (Leroy et al., 2011), and f. The Early Pleistocene (Gelasian-Calabrian Transition) theoretical model (Combourieu Nebout et al., 1993). The dots represent the dominant vegetation. Their presence allows us to visualise the local vegetation.

by temperate forest expansion; the Gelasian-Calabrian model displays a subtropical forest linked to warmer and more humid conditions related to its older age. The transition from interglacials to glacials follows a similar pattern across all sites, marked by the expansion of high-altitude conifer forests. In the OPD 976 record, a brief Ericaceae phase preceding conifer development may reflect the initial onset of colder, yet still humid conditions (Fig. 7a). This short Ericaceae phase could be attributed to the site's specific longitudinal and/or altitudinal position, resulting in slightly different climatic conditions.

In contrast, different vegetation patterns occur during glacial to interglacial transitions: OPD 976 and Montalbano Jonico and Ohrid are marked by coniferous forest development during the transitions,

expressed by two different families, Cupressaceae (*Cupressus/Juniperus* type) and Pinaceae in the ODP 976 and Ohrid records, respectively. This difference can be explained by more arid conditions in the southern Mediterranean and wetter conditions in the Balkan Mountains. This transition is not recorded in Tenaghi Philippon, probably due to the catchment's altitudinal position, very high proportions of open vegetation and the fact that there are no forests located in proximity to the basin. In effect, the transition phase is less marked than at the other sites. The theoretical patterns of the Early-Middle Pleistocene and that of the Gelasian - Calabrian transition are also quite different for this transition: respectively an open vegetation and a deciduous forest, undoubtedly linked for the first to the choice of sites covering a longer period of time (1.8–0.8 Ma) and to higher latitudes (most of them being above 40°N), and for the second to the age of this site (~1.8 Ma).

5.1.3. Vegetation and climate responses to orbital parameters

Between 1.25 and 1.06 Ma, interglacial periods are marked by low precession and maximum summer insolation values, except during MIS 33 (1114–1104 ka). The pattern during MIS 31 ("the super interglacial" with high obliquity and eccentricity and precession minima leading to some of the highest summer insolation levels of the Pleistocene), recorded in the Alboran Sea has already been documented in the Atlantic area (core U1385) (Oliveira et al., 2017). However, in the ODP 976 core, this interglacial does not appear to be the one with the highest percentage of temperate taxa with a mean of 26 % against 30, 27 and 35 % for the MIS 33, 35 and 35 respectively. Instead it shows the greatest diversity of deciduous forest trees (Fig. 5).

The Early Pleistocene is a period during which climatic cycles have a periodicity of 41 ka, driven by obliquity (Ruddiman et al., 1986; Head and Gibbard, 2015; Barker et al., 2022). Between MIS 37 and 31, glacial periods are all equivalent in duration (~25 kyr), but this is not the case for interglacial periods: MIS 33 is short (~10 kyr), while MIS 35 is very long (~50 kyr) (Lisiecki and Raymo, 2005). The MIS 35-34 and the MIS 36-35 cycles are anomalously long, respectively lasting for 75.1 kyr and 75.3 kyr (Shackleton et al., 1990; Lisiecki, 2010; Barker et al., 2022; Margari et al., 2023). This duration may be due to a greater eccentricity influence. At site ODP 976, the MIS 36, MIS 34 and MIS 32 glacial periods show the lowest occurrence of temperate taxa and the highest expansion of steppe taxa. However, MIS 34 maintains these glacial conditions for longer. These results are consistent with the hypothesis of an extreme cooling during MIS 34, triggered by an eccentricity minimum (Margari et al., 2023), and anomalous variations in insolation and precession (Fig. 5).

5.2. Relict taxa history between 1.25 and 1.06 Ma in the Mediterranean area

From the Pliocene to the EMPT, the vegetation in the Mediterranean area changed considerably. Subtropical forests were replaced by temperate forests dominated by oaks and high-altitude conifers. In parallel, steppes dominated by *Artemisia* and *Ephedra* developed progressively during glacial periods (Suc, 1984; Combourieu Nebout, 1993; Bertini, 2003; Magri et al., 2017). Temperate relict taxa such as *Carya*, *Pterocarya*, *Tsuga* and the mesophilous *Cathaya* began to decline at the onset of the EMPT (Bertini, 2003; González-Sampériz et al., 2010; Orain et al., 2013; Magri et al., 2017; Donders et al., 2021).The subtropical plant *Engelhardia* and the temperate taxa: *Eucommia, Liquidambar* and *Parrotia* disappeared progressively during the Early Pleistocene (González-Sampériz et al., 2010; Magri et al., 2017). Most of these relict taxa are found today in Asia in subtropical to temperate regions (Table 3).

Magri et al. (2017) addressed the challenge to use the last occurrence and/or abundance of taxa as bio-stratigraphic markers and the difficulties in identifying rare taxa when counts are not sufficiently detailed. Furthermore, some sites only cover a short period of time (extending over a few MIS), which makes it impossible to obtain continuous information on the different extinction phases: the Pliocene-Pleistocene transition, the Gelasian-Calabrian transition and MIS 16 and 12 (Magri et al., 2017). ODP 976 is therefore of considerable interest for the continuous study of vegetation dynamics and extinction over time. Previous studies on ODP 976 suggested the occurrence of temperate taxa: *Carya*, *Cathaya,* and subtropical taxa:*Engelhardia*, *Rhoiptelea*, *Taxodium* and *Tsuga* during MIS 20 and 19, *Pterocarya* during MIS 31 and 23, *Tsuga* during MIS 30, 26, 23, 20 and 19 and *Zelkova* in MIS 31, 25, 20 and 19 (Joannin et al., 2011; Toti et al., 2020). Here, during MIS 37 to 31, *Carya, Pterocarya* and *Zelkova* are present in mesothermic formations at mid and low altitudes, while *Cathaya* and *Tsuga* are present in high-altitude conifer forests (Table 3). It is of note that the low number of and/or very sporadic relict taxa in ODP 976 may be due to the distance from the rare and distant refugia where relict taxa may still have persisted during the studied period (Figs. 4 and 8). The nearby Spanish Palominas sequence also records few relict taxa (e.g., *Eucommia* and *Parrotia*), which reinforced our interpretation (Fig. 8). *Carya, Zelkova, Eucommia and Pterocarya* are present in the palynological analysis of the Barranco Leon 3 archaeological site (~1.2 Ma; Ochando et al., 2022), attesting to the persistence of some temperate relict taxa in the south of the Iberian Peninsula at the end of the Early Pleistocene.

Other Mediterranean sites (Palominas, Monte San Giorgio, Tenaghi

Table 3
Current ecology and location of the relict taxa observed during the EMPT in the Mediterranean basin. T_A: Mean annual temperature, P_A: total annual precipitation, N: North, S: South, E: East, W: West and C: central.[1] Mabberley (1997),[2] Fauquette et al. (1998),[3] Orain et al. (2013),[4] Magri et al. (2017),[5] Fang et al. (2011),[6] Meng et al. (2015),[7] Wang et al. (2003),[8] Zhang and Turland (2003),[9] Öztürk et al. (2008),[10] Sefidi et al. (2011),[11] Li and Del Tredici (2008),[12] Akhani and Salimian (2003),[13] (https://www.conifers.org),[14] Biltekin et al. (2015),[15] Magri (2012).

Taxa	Family	Current distribution[1]	Altitude (m)	Biomes	T_A (°C)[2]	P_A (mm)[2]
Carya	Juglandaceae	N to C America, E Asia	<1000[3]	Subtropical and temperate continental Maritime influence[3]	4–26	50–3000
Cathaya	Pinaceae	W China	900–1900[4]	Mesophilous forest[4]	10–20	1000–1600
Engelhardia	Juglandaceae	Himalaya to Malaysia	<2000[4]	Tropical to subtropical forests[4,5,6]	12–25	740–3500[4]
Eucommia	Eucommiaceae	China	200–1700[7]	Mixed forests, lower mountains, ridges, valleys, dry ravines[8]		
Liquidambar	Altingiaceae	E Mediterranean E Asia, S, E, N & C America	<1000[9]	Temperate forest[9] Wet bioclimate[4]	10–25	700–2200
Parrotia	Hamamelidaceae	SW Caspian (*P. persica*), E China (*P. subaequalis*)	150-700 (Iran)[10]	Deciduous forest[10,11]	14–22	300–1500
Pterocarya	Juglandaceae	Caucasia to E. and SE Asia	<1000[12]	Flooded forest valleys with running water[4]	9–25	240–1960
Sciadopitys	Sciadopityaceae	C & S Japan	500–1000[13]	Mixed cloud forest	5–15	1000–2500
Taxodium	Cupressaceae	EN America, Mexican highland		Riparian and wetland habitats[13]	16–25	1100–2400
Tsuga	Pinaceae	N America, E Asia to Vietnam	<3800[4]	Subalpine coniferous, temperate deciduous forests[4]	0–15	700–4500[4]
Zelkova	Ulmaceae	Crete, W&E Asia		Riparian[14]	8.5–25	250–1400
Cedrus	Pinaceae	N Africa (*C.atlantica*) to Asia (*C.libani*)	1300–2600[15]	Mediterranean conifer forest[15]	7–18	500–1500

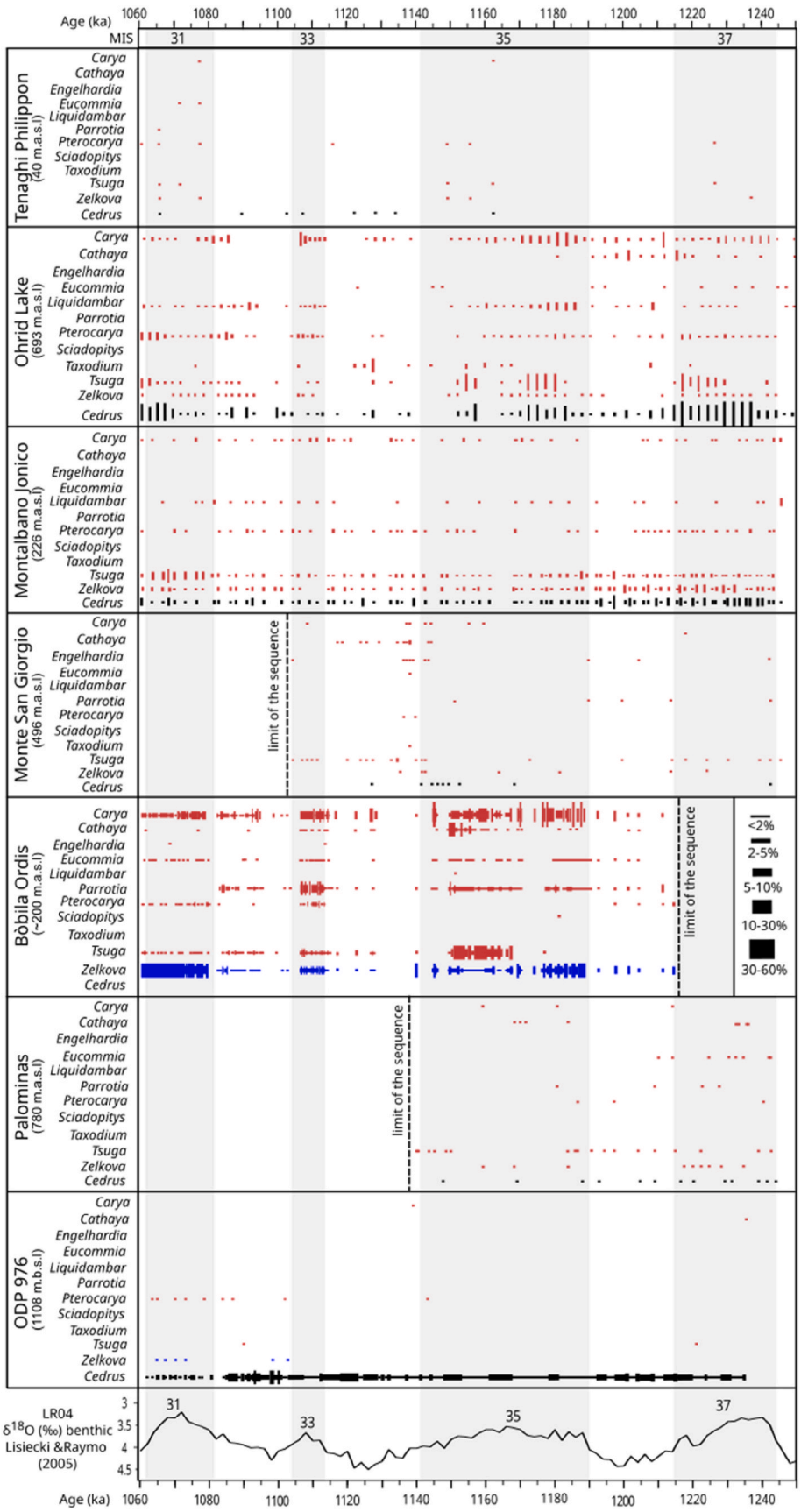

Fig. 8. Relict taxa recorded in late Early Pleistocene pollen records around the Mediterranean region. Red lines represent the percentages of relict taxa, blue lines correspond to taxa with uncertain pollen identification (e.g., *Ulmus/Zelkova*), black lines show *Cedrus* percentages.

Philipon, and OPD 976) document low percentages of relict taxa (Fig. 8), perhaps due to their location in the south of the Mediterranean basin, south of or around 40°N and at low altitudes. In contrast, relict taxa are better represented at Bòbila Ordis and Lake Orhid, sites situated at higher latitudes or altitudes, respectively. This is probably due to less pronounced drought in these regions, especially during interglacials, as shown by the increase in forest cover during these temperate periods and by model simulations (Leroy, 2008; Wagner et al., 2019; Donders et al., 2021). However, the Montalbano Jonico record shows the continuous presence of relict taxa, although it is situated around 40°N, which can be explained by less marked fluctuations between interglacial and glacial periods (Figs. 7 and 8; Joannin et al., 2011). This gradient contradicts the common view that suggests taxa persist longer in southern European regions and highlights their southernmost boundary of tolerance to arid conditions. However, it is necessary to take into account the origin of the sediments in some of these sequences (ODP 976, Montalbano and Monte San Giorgio), which are of marine origin and may cause dilution of the signal from these relict taxa compared to the main taxa.

The presence of *Cedrus* in the Iberian Peninsula during the Late Pleistocene is still debated (González-Sampériz et al., 2010; Joannin et al., 2011; Magri, 2012; Magri et al., 2017; Suc et al., 2018). In the ODP 976 record, at the end of the Early Pleistocene (from MIS 31 to 23), *Cedrus* pollen probably comes from both northern Africa and southern Spain (Joannin et al., 2011). A comparison between Palominas and the ODP 976 sequences (Fig. 8) shows that *Cedrus* was nearly absent from the continental record, and we may thus assume that most of the *Cedrus* pollen grains evidenced in the ODP marine sequence originate from northern Morocco, as suggested by Magri (2012). The species *Cedrus atlantica* is still present today in north-western Africa. Nevertheless, we cannot rule out the possibility that some *Cedrus* pollen grains came from the last refugia of *Cedrus* in southern Spain (Postigo Mijarra et al., 2007). On the other hand, the significant presence of *Cedrus* at the Ohrid and Montalbano sites (Fig. 8) may be linked to the ancient expansion of *Cedrus libani* and *C. brevifolia*. These latter two species may still have been present before their distribution area moved eastwards to Türkiye and the Levant, where they are still present today.

6. Conclusion

New high-resolution isotope and pollen data from the ODP Site 976 fill the gap of records, providing insights into environmental changes at the beginning of the Early-Mid Pleistocene Transition. The sea surface isotope record in the Alboran Sea contributed to a better definition of the chronology of the core from MIS 37 to MIS 31 and, alongside pollen data, both proxies fully mimic the cold/warm glacial/interglacial oscillations. This marine archive records regional vegetation in southern Spain and northern Morocco without quantifying the contribution of each of these two pollen sources. Nevertheless, the ODP 976 vegetation record seems to indicate the lengthening of glacial/interglacial cycles from 41 to 100 kyr, within a MIS35-34 cycle duration of 76 kyr. MIS 34, with its prolonged low values of temperate elements and high values of steppe taxa, testifies to a particularly cold glacial period linked to a disruption in summer boreal insolation.

The corpus of Mediterranean sites reveals that the vegetation dynamics during glacial/interglacial cycles can be characterized by four phases: 1) Conifer formations during glacial/interglacial transitions, 2) deciduous forests (mainly *Quercus*) during warm and wet interglacial periods, 3) heaths and high-altitude coniferous forests throughout interglacial/glacial transitions, 4) steppe expansion during cold and arid glacial periods. Nevertheless, during the glacial to interglacial transition the conifer type change around the Mediterranean due to the influence of Mediterranean vegetation. Only the significant presence of Ericaceae distinguishes the ODP 976 record from the others and brings it closer to the data found off the coast of Portugal. This presence, mainly in the western Mediterranean, is strongly linked to the Atlantic humidity carried by the westerlies. Available pollen data confirms a more limited development of relict taxa south of 40°N, likely tied to a north-south gradient in aridity and question the traditional view of southern refugia.

Data statement

Data are available upon request by email.

Author contributions

This article is the result of teamwork by a palynologist, a micropaleontologist and a geochemist on this ODP 976 sequence. Pollen analyses were carried out by M. Catrain. Pollen and foraminiferal extraction treatments and isotopic data analyses were conducted by L. Dubost, J. Lepelletier, E. Paquier Comas, M. Fries and P. Richard. S. Joannin and J.-P. Suc provided the other ODP 976 data and the unpublished data of Monte San Giorgio. The manuscript was written by M. Catrain with the substantial contribution of N. Combourieu-Nebout and V. Lebreton. All coauthors shared their expertise and contributed to the writing of this paper.

Funding

This work was supported by ERC project LATEUROPE project [n°101052653]

Declaration of competing interest

The authors declare no competing financial interests.

Acknowledgements

We are grateful to the ERC LATEUROPE project (n°101052653), the Centre National de la Recherche Scientifique (CNRS) and the Museum National d'Histoire Naturelle (MNHN) for their financial support. We thank the PANOPLY analytical platform at LSCE for facilities to carry out isotopic measurements and the Ocean Drilling Program (ODP) for making the material from the core ODP leg 161 Site 976 available. We would also like to thank Yul Altolaguirre, Suzanne Leroy and Jörg Pross for sharing and giving us permission to use their data. This is an ISEM publication n° 2025-194. We thank the editor Yan Zhao and the two anonymous reviewers whose relevant comments helped significantly improve the manuscript quality.

Data availability

Data will be made available upon request to the corresponding author.

References

Akhani, H., Salimian, M., 2003. An extant disjunct stand of *Pterocarya fraxinifolia (Juglandaceae)* in the central Zagros Mountains, W Iran[1]. Willdenowia 33, 113–120. https://doi.org/10.3372/wi.33.33111.

Altolaguirre, Y., Bruch, A.A., Gibert, L., 2020. A long early pleistocene pollen record from baza basin (SE Spain): major contributions to the palaeoclimate and palaeovegetation of southern Europe. Quat. Sci. Rev. 231, 106199. https://doi.org/10.1016/j.quascirev.2020.106199.

Altolaguirre, Y., Postigo-Mijarra, [J.M.a], Barrón, E., Carrión, J.S., Leroy, S.A.G., Bruch, A. A., 2019. An environmental scenario for the earliest hominins in the Iberian Peninsula: early Pleistocene palaeovegetation and palaeoclimate. Rev. Palaeobot. Palynol. 260, 51–64. https://doi.org/10.1016/j.revpalbo.2018.10.008.

Altolaguirre, Y., Schulz, M., Gibert, L., Bruch, A.A., 2021. Mapping Early Pleistocene environments and the availability of plant food as a potential driver of early Homo presence in the Guadix-Baza Basin (Spain). J. Hum. Evol. 155, 102986. https://doi.org/10.1016/j.jhevol.2021.102986.

Andrieu-Ponel, V., Rochette, P., Demory, F., Alçiçek, H., Boulbes, N., Bourlès, D., Helvacı, C., Lebatard, A.-E., Mayda, S., Michaud, H., Moigne, A.-M., Nomade, S., Perrin, M., Ponel, P., Rambeau, C., Vialet, A., Gambin, B., Alçiçek, M.C., 2021. Continuous presence of proto-cereals in Anatolia since 2.3 Ma, and their possible co-

evolution with large herbivores and hominins. Sci. Rep. 11, 8914. https://doi.org/10.1038/s41598-021-86423-8.
Barker, S., Starr, A., Conn, S., Lordsmith, S., Owen, L., Nederbragt, A., Hemming, S., Hall, I., Levay, L., 2022. Persistent influence of precession on northern ice sheet variability since the early Pleistocene. Science 376, 961–967. https://doi.org/10.1126/science.abm4033.
Beaudouin, C., Suc, J.-P., Escarguel, G., Arnaud, M., Charmasson, S., 2007. The significance of pollen signal in present-day marine terrigenous sediments: the example of the Gulf of Lions (western Mediterranean Sea). Geobios 40, 159–172. https://doi.org/10.1016/j.geobios.2006.04.003.
Benabid, A., 1985. Les écosystèmes forestiers, préforestiers et presteppiques du Maroc : diversité, répartition biogéographique et problèmes posés par leur aménagement. Forêt Méditerranéenne VII, pp. 53–64.
Benítez-Benítez, C., Escudero, M., Rodríguez-Sánchez, F., Martín-Bravo, S., Jiménez-Mejías, P., 2018. Pliocene–Pleistocene ecological niche evolution shapes the phylogeography of a Mediterranean plant group. Mol. Ecol. 27, 1696–1713. https://doi.org/10.1111/mec.14567.
Berger, A., Loutre, M.F., 1991. Insolation values for the climate of the last 10 million years. Quat. Sci. Rev. 10, 297–317. https://doi.org/10.1016/0277-3791(91)90033-Q.
Bertini, A., 2003. Early to Middle Pleistocene changes of the Italian flora and vegetation in the light of a chronostratigraphic framework. IL Quaternario Italian Journal of Quaternary Sciences 16, 19–36.
Bertini, A., Combourieu-Nebout, N., 2023. Piacenzian to late Pleistocene flora and vegetation in Italy: a moving sketch. Alpine and Mediterranean Quaternary 36, 91–119. https://doi.org/10.26382/AMQ.2023.05.
Beug, H.-J., 2004. Leitfaden der Pollenbestimmung für Mitteleuropa und angrenzende Gebiete. Verlag Dr. Friedrich Pfeil, München.
Biltekin, D., Popescu, S.-M., Suc, J.-P., Quézel, P., Jiménez-Moreno, G., Yavuz, N., Çağatay, M.N., 2015. Anatolia: a long-time plant refuge area documented by pollen records over the last 23million years. Rev. Palaeobot. Palynol. 215, 1–22. https://doi.org/10.1016/j.revpalbo.2014.12.004.
Carbonell, E., Bermúdez De Castro, J.M., Parés, J.M., Pérez-González, A., Cuenca-Bescós, G., Ollé, A., Mosquera, M., Huguet, R., Van Der Made, J., Rosas, A., Sala, R., Vallverdú, J., García, N., Granger, D.E., Martinón-Torres, M., Rodríguez, X.P., Stock, G.M., Vergès, J.M., Allué, E., Burjachs, F., Cáceres, I., Canals, A., Benito, A., Díez, C., Lozano, M., Mateos, A., Navazo, M., Rodríguez, J., Rosell, J., Arsuaga, J.L., 2008. The first hominin of Europe. Nature 452, 465–469. https://doi.org/10.1038/nature06815.
Castroviejo, S., Aedo, C., Cirujano, S., Laínz, M., Montserrat, P., Morales, R., Muñoz Garmendia, F., Navarro, C., Paiva, J., Soriano, C., 1993. Ericaceae. In: Flora Iberica, pp. 514–523. Madrid.
Clark, P.U., Archer, D., Pollard, D., Blum, J.D., Rial, J.A., Brovkin, V., Mix, A.C., Pisias, N. G., Roy, M., 2006. The middle Pleistocene transition: characteristics, mechanisms, and implications for long-term changes in atmospheric pCO2. Quaternary Science Reviews, Critical Quaternary Stratigraphy 25, 3150–3184. https://doi.org/10.1016/j.quascirev.2006.07.008.
Site 976. In: Comas, M.C., Zahn, R., Klaus, A. (Eds.), 1996. Proceedings of the Ocean Drilling Program, Initial Reports, pp. 179–297.
Combourieu Nebout, N., 1993. Vegetation response to upper Pliocene glacial/interglacial cyclicity in the central mediterranean. Quaternary Research 40, 228–236.
Combourieu Nebout, N., Londeix, L., Baudin, F., Turon, J.L., von Grafenstein, R., Zahn, Rainer, 1999. Quaternary marine and continental paleoenvironments in the western Mediterranean (site 976, Alboran Sea): palynological evidence. In: Zahn, R., Comas, M.C., Klaus, A. (Eds.), Proceedings of the Ocean Drilling Program, 161 Scientific Results, Proceedings of the Ocean Drilling Program. Ocean Drilling Program, pp. 457–468. https://doi.org/10.2973/odp.proc.sr.161.1999.
Combourieu-Nebout, N., Bertini, A., Russo-Ermolli, E., Peyron, O., Klotz, S., Montade, V., Fauquette, S., Allen, J., Fusco, F., Goring, S., Huntley, B., Joannin, S., Lebreton, V., Magri, D., Martinetto, E., Orain, R., Sadori, L., 2015. Climate changes in the central Mediterranean and Italian vegetation dynamics since the Pliocene. Rev. Palaeobot. Palynol. 218, 127–147. https://doi.org/10.1016/j.revpalbo.2015.03.001.
De Deckkers, P., Geurts, M.A., Julia, R., 1979. Seasonal rhythmites from a lower pleistocene lake in northeastern sapin. Palaeogeogr. Palaeoclimatol. Palaeoecol. 26, 43–71.
De Kaenel, E., Siesser, W., Murat, A., 1999. Pleistocene calcareous nannofossil biostratigraphy and the Western Mediterranean sapropels, Sites 974 to 977 and 979. In: Proceedings of the Ocean Drilling Program, vol. 161. Scientific Results. https://doi.org/10.2973/odp.proc.sr.161.250.1999.
Donders, T., Panagiotopoulos, K., Koutsodendris, A., Bertini, A., Mercuri, A.M., Masi, A., Combourieu-Nebout, N., Joannin, S., Kouli, K., Kousis, I., Peyron, O., Torri, P., Florenzano, A., Francke, A., Wagner, B., Sadori, L., 2021. 1.36 million years of Mediterranean forest refugium dynamics in response to glacial–interglacial cycle strength. Proc. Natl. Acad. Sci. 118, e2026111118. https://doi.org/10.1073/pnas.2026111118.
Dubois, J.-M., 2001. Cycles climatiques des paramètres orbitaux vers 1Ma. Etude de la coupe de Monte San Giorgio (Caltagirone, Sicile) : palynologie, isotopes stables. calcimétrie. Université Claude Bernard-Lyon 1. Lyon.
Fabres, J., Calafat, A., Sanchez-Vidal, A., Canals, M., Heussner, S., 2002. Composition and spatio-temporal variability of particle fluxes in the western alboran gyre, Mediterranean Sea. Journal of Marine Systems, MATER: MAss Transfer and Ecosystem Response 33–34, 431–456. https://doi.org/10.1016/S0924-7963(02)00070-2.
Fang, J., Wang, Z., Tang, Z., 2011. Atlas of Woody Plants in China: Distribution and Climate. Springer Science & Business Media.
Fauquette, S., Guiot, J., Suc, J.-P., 1998. A method for climatic reconstruction of the Mediterranean Pliocene using pollen data. Palaeogeogr. Palaeoclimatol. Palaeoecol. 144, 183–201. https://doi.org/10.1016/S0031-0182(98)00083-2.
Fletcher, W.J., Sánchez Goñi, M.F., 2008. Orbital- and sub-orbital-scale climate impacts on vegetation of the western Mediterranean basin over the last 48,000 yr. Quat. res. 70, 451–464. https://doi.org/10.1016/j.yqres.2008.07.002.
Fubelli, G., Falcucci, E., Mei, A., Dramis, F., 2008. Evoluzione quaternaria del Bacino di Leonessa (Rieti). Il Quat. 21, 457–468.
Fusco, F., 2007. Vegetation response to early Pleistocene climatic cycles in the Lamone valley (Northern Apennines, Italy). Rev. Palaeobot. Palynol. 145, 1–23. https://doi.org/10.1016/J.REVPALBO.2006.08.005.
GeMiNa, 1962. Ligniti e Torbe dell'Italia Continentale., Società Geomineraria Nazionale, ILTE Ed. Roma, Italia.
Geurts, M.A., 1977. Premières données a l'étude palynologique des dépôt calcareux quaternaire en Catalogne. Acta geologica hispanica XII, 86–89.
González-Donoso, J.M., Serrano, F., Linares, D., 2000. Sea surface temperature during the quaternary at ODP sites 976 and 975 (western mediterranean). Palaeogeogr. Palaeoclimatol. Palaeoecol. 162, 17–44. https://doi.org/10.1016/S0031-0182(00)00103-6.
González-Sampériz, P., Leroy, S.A.G., Carrión, J.S., Fernández, S., García-Antón, M., Gil-García, M.J., Uzquiano, P., Valero-Garcés, B., Figueiral, I., 2010. Steppes, savannahs, forests and phytodiversity reservoirs during the Pleistocene in the Iberian Peninsula. Rev. Palaeobot. Palynol. 162, 427–457. https://doi.org/10.1016/j.revpalbo.2010.03.009.
Grimm, E., 1991. TILIA and TILIA GRAPH Computer Programs. Illinois State Museum, Springfield.
Guerzoni, S., Molinaroli, E., Chester, R., 1997. Saharan dust inputs to the western Mediterranean Sea: depositional patterns, geochemistry and sedimentological implications. Deep Sea Res. Part II Top. Stud. Oceanogr. 44, 631–654. https://doi.org/10.1016/S0967-0645(96)00096-3.
Head, M.J., Gibbard, P.L., 2015. Early–Middle Pleistocene transitions: linking terrestrial and marine realms. Quat. Int. 389, 7–46. https://doi.org/10.1016/j.quaint.2015.09.042.
Herbert, T.D., 2023. The mid-pleistocene climate transition. Annu. Rev. Earth Planet Sci. 51, 389–418. https://doi.org/10.1146/annurev-earth-032320-104209.
Heusser, L.E., 1988. Pollen distribution in marine sediments on the continental margin off northern California. Mar. Geol. 80, 131–147. https://doi.org/10.1016/0025-3227(88)90076-X.
Huguet, R., Rodríguez-Álvarez, X.P., Martinón-Torres, M., Vallverdú, J., López-García, J. M., Lozano, M., Terradillos-Bernal, M., Expósito, I., Ollé, A., Santos, E., Saladié, P., De Lombera-Hermida, A., Moreno-Ribas, E., Martín-Francés, L., Allué, E., Núñez-Lahuerta, C., Van Der Made, J., Galán, J., Blain, H.-A., Cáceres, I., Rodríguez-Hidalgo, A., Bargalló, A., Mosquera, M., Parés, J.M., Marín, J., Pineda, A., Lordkipanidze, D., Margveslashvili, A., Arsuaga, J.L., Carbonell, E., Bermúdez De Castro, J.M., 2025. The earliest human face of Western Europe. Nature. https://doi.org/10.1038/s41586-025-08681-0.
Joannin, S., Bassinot, F., Nebout, N.C., Peyron, O., Beaudouin, C., 2011. Vegetation response to obliquity and precession forcing during the Mid-Pleistocene Transition in Western Mediterranean region (ODP site 976). Quat. Sci. Rev. 30, 280–297. https://doi.org/10.1016/j.quascirev.2010.11.009.
Joannin, S., Ciaranfi, N., Stefanelli, S., 2008. Vegetation changes during the late early pleistocene at Montalbano Jonico (province of matera, southern Italy) based on pollen analysis. Palaeogeogr. Palaeoclimatol. Palaeoecol. 270, 92–101. https://doi.org/10.1016/j.palaeo.2008.08.017.
Julià Bruguès, R., Suc, J.-P., 1980. Analyse pollinique des dépôts lacustresdu Pléistocène inférieur de Banyoles (Bañolas, site de la Bòbila Ordis - Espagne): un élément nouveau dans la reconstitution de l'histoire paléoclimatique des régions méditerranéennes d'Europe occidentale. Geobios 13, 5–19.
Köppen, W., 1936. Das geographische System der Klimate. In: Köppen, W., Geiger, R. (Eds.), Handbuch der Klimatologie. Verlag von Gebrüder Borntl'aeger, Berlin, p. 44.
Laskar, J., Robutel, P., Joutel, F., Gastineau, M., Correia, A.C.M., Levrard, B., 2004. A long-term numerical solution for the insolation quantities of the Earth. A&A 428, 261–285. https://doi.org/10.1051/0004-6361:20041335.
Lebreton, V., 2004. Paysages et climats contemporains des premiers hominigés en Italie. Analyse pollinique des sites du Pléistocène Inférieur et moyen de Ca' Belvedere di Monte Poggiolo (Forli, Emilie-Romagne) et de la Pineta (Isernia, Molise). Muséum National d'Histoire Naturelle, Paris.
Leroy, S.A.G., 2008. Vegetation cycles in a disturbed sequence around the Cobb-Mountain subchron in Catalonia (Spain). J. Paleolimnol. 40, 851–868. https://doi.org/10.1007/s10933-008-9203-9.
Leroy, S.A.G., 2007. Progress in palynology of the gelasian–calabrian stages in Europe: ten messages. Rev. Micropaleontol. 50, 293–308. https://doi.org/10.1016/j.revmic.2006.08.001.
Leroy, S.A.G., 1988. Image pollinique d'une steppe du Pliocène supérieur à Bobila Ordis, Banyoles (Catalogne), vol. XXV. Institut français de Pondichéry, pp. 197–207.
Leroy, S.A.G., Ambert, P., Suc, J.-P., 1994. Pollen record of the Saint-Macaire maar (Hérault, southern France) : a lower Pleistocene glacial phase in the Languedoc costal plain. Rev. Palaeobot. Palynol. 80, 149–157.
Leroy, S.A.G., Arpe, K., Mikolajewicz, U., 2011. Vegetation context and climatic limits of the Early Pleistocene hominin dispersal in Europe. Quat. Sci. Rev. 30, 1448–1463. https://doi.org/10.1016/j.quascirev.2010.01.017.
Li, J., Del Tredici, P., 2008. The Chinese Parrotia: a sibling species of the Persian Parrotia. Arnoldia. The Magazine of the Arnold Arboretum 66, 2–9.
Lisiecki, L.E., 2010. Links between eccentricity forcing and the 100,000-year glacial cycle. Nature Geosci 3, 349–352. https://doi.org/10.1038/ngeo828.

Lisiecki, L.E., Raymo, M.E., 2005. A Pliocene-Pleistocene stack of 57 globally distributed benthic δ18O records. Paleoceanography 20. https://doi.org/10.1029/2004PA001071.

Lourens, L.J., 2004. Revised tuning of Ocean Drilling Program Site 964 and KC01B (Mediterranean) and implications for the δ18O, tephra, calcareous nannofossil, and geomagnetic reversal chronologies of the past 1.1 Myr. Paleoceanography 19. https://doi.org/10.1029/2003PA000997.

Mabberley, D.J., 1997. The Plant-Book. A Portable Dictionary of the Vascular Plants, second ed. Cambridge University Press.

Macias, D., Garcia-Gorriz, E., Stips, A., 2016. The seasonal cycle of the Atlantic Jet dynamics in the Alboran Sea: direct atmospheric forcing versus Mediterranean thermohaline circulation. Ocean Dyn. 66, 137–151. https://doi.org/10.1007/s10236-015-0914-y.

Magri, D., 2012. Quaternary history of Cedrus in south Europe. Annali di Botanica 0. https://doi.org/10.4462/annbotrm-10022.

Magri, D., Di Rita, F., Aranbarri, J., Fletcher, W., González-Sampériz, P., 2017. Quaternary disappearance of tree taxa from Southern Europe: timing and trends. Quat. Sci. Rev. 163, 23–55. https://doi.org/10.1016/j.quascirev.2017.02.014.

Magri, D., Rita, F.D., Palombo, M.R., 2010. An Early Pleistocene interglacial record from an intermontane basin of central Italy (Scoppito, L'Aquila). Quat. Int. 225, 106–113. https://doi.org/10.1016/j.quaint.2009.04.005.

Margari, V., Hodell, D.A., Parfitt, S.A., Ashton, N.M., Grimalt, J.O., Kim, H., Yun, K.-S., Gibbard, P.L., Stringer, C.B., Timmermann, A., Tzedakis, P.C., 2023. Extreme glacial cooling likely led to hominin depopulation of Europe in the Early Pleistocene. Science 381, 693–699. https://doi.org/10.1126/science.adf4445.

Martinetto, E., Bertini, A., Basilici, G., Baldanza, A., Bizzarri, R., Cherin, M., Gentili, S., Pontini, M.R., 2014. The plant record of the Dunarobba and Pietrafitta sites in the Plio-Pleistocene paleoevnvironmental context of central Italy. Alpine and Mediterranean Quaternary 27, 29–72.

Médail, F., 2022. Plant biogeography and vegetation patterns of the mediterranean Islands. Bot. Rev. 88, 63–129. https://doi.org/10.1007/s12229-021-09245-3.

Meng, H.-H., Su, T., Huang, Y.-J., Zhu, H., Zhou, Z.-K., 2015. Late Miocene Palaeocarya (Engelhardieae: Juglandaceae) from southwest China and its biogeographic implications. J. Systemat. Evol. 53, 499–511. https://doi.org/10.1111/jse.12145.

Moreno, A., Cacho, I., Canals, M., Grimalt, J.O., Sánchez-Goñi, M.F., Shackleton, N., Sierro, F.J., 2005. Links between marine and atmospheric processes oscillating on a millennial time-scale. A multi-proxy study of the last 50,000yr from the Alboran Sea (Western Mediterranean Sea). Quaternary Science Reviews, Quaternary Land-ocean Correlation 24, 1623–1636. https://doi.org/10.1016/j.quascirev.2004.06.018.

Moyano, I.T., Barsky, D., Cauche, D., Celiberti, V., Grégoire, S., Lebegue, F., Moncel, M. H., De Lumley, H., 2011. The archaic stone tool industry from Barranco León and Fuente Nueva 3, (Orce, Spain): evidence of the earliest hominin presence in southern Europe. Quat. Int. 243, 80–91. https://doi.org/10.1016/j.quaint.2010.12.011.

Murat, A., 1999. Pliocene–Pleistocene occurrence of sapropels in the western Mediterranean sea and their relation to eastern Mediterranean sapropels, Proceedings of the Ocean Drilling Program. Ocean Drilling Program. https://doi.org/10.2973/odp.proc.sr.161.1999.

Ochando, J., Carrión, J., Altolaguirre, Y., Munuera, M., Amorós, G., Jiménez-Moreno, G., Solano-García, J., Barsky, D., Luzón, C., Sánchez-Bandera, C., Serrano-Ramos, A., Toro-Moyano, I., Saarinen, J., Blain, H.-A., Bocherens, H., Oms, O., Agustí, J., Fortelius, M., Jiménez-Arenas, J.M., 2022. Palynological investigations in the orce archaeological zone, early pleistocene of southern Spain. Rev. Palaeobot. Palynol. 304, 104725. https://doi.org/10.1016/j.revpalbo.2022.104725.

Oliveira, D., Sánchez Goñi, M.F., Naughton, F., Polanco-Martínez, J.M., Jimenez-Espejo, F.J., Grimalt, J.O., Martrat, B., Voelker, A.H.L., Trigo, R., Hodell, D., Abrantes, F., Desprat, S., 2017. Unexpected weak seasonal climate in the western Mediterranean region during MIS 31, a high-insolation forced interglacial. Quat. Sci. Rev. 161, 1–17. https://doi.org/10.1016/j.quascirev.2017.02.013.

Orain, R., Lebreton, V., Ermolli, E.R., Combourieu-Nebout, N., Sémah, A.-M., 2013. Carya as marker for tree refuges in southern Italy (Boiano basin) at the Middle Pleistocene. Palaeogeogr. Palaeoclimatol. Palaeoecol. 369, 295–302. https://doi.org/10.1016/j.palaeo.2012.10.037.

Ozenda, P., 1994. Végétation du continent européen. Delachaux et Niestlé.

Öztürk, M., Çelik, A., Güvensen, A., Hamzaoğlu, E., 2008. Ecology of tertiary relict endemic Liquidambar orientalis Mill. forests. For. Ecol. Manag. 256, 510–518. https://doi.org/10.1016/j.foreco.2008.01.027.

Panagiotopoulos, K., Holtvoeth, J., Kouli, K., Marinova, E., Francke, A., Cvetkoska, A., Jovanovska, E., Lacey, J.H., Lyons, E.T., Buckel, C., Bertini, A., Donders, T., Just, J., Leicher, N., Leng, M.J., Melles, M., Pancost, R.D., Sadori, L., Tauber, P., Vogel, H., Wagner, B., Wilke, T., 2020. Insights into the evolution of the young Lake Ohrid ecosystem and vegetation succession from a southern European refugium during the Early Pleistocene. Quat. Sci. Rev. 227, 106044. https://doi.org/10.1016/j.quascirev.2019.106044.

Peel, M.C., Finlayson, B.L., McMahon, T.A., 2007. Updated world map of the Köppen-Geiger climate classification. Hydrol. Earth Syst. 11, 1633–1644. https://doi.org/10.5194/hess-11-1633-2007.

Pérez-Folgado, M., Sierro, F.J., Flores, J.A., Cacho, I., Grimalt, J.O., Zahn, R., Shackleton, N., 2003. Western Mediterranean planktonic foraminifera events and millennial climatic variability during the last 70 kyr. Mar. Micropaleontol. 48, 49–70. https://doi.org/10.1016/S0377-8398(02)00160-3.

Popescu, S.-M., Biltekin, D., Winter, H., Suc, J.-P., Melinte-Dobrinescu, M.C., Klotz, S., Rabineau, M., Combourieu-Nebout, N., Clauzon, G., Deaconu, F., 2010. Pliocene and Lower Pleistocene vegetation and climate changes at the European scale: long pollen records and climatostratigraphy. Quat. Int. 219, 152–167. https://doi.org/10.1016/j.quaint.2010.03.013.

Postigo Mijarra, J.M., Burjachs, F., Gómez Manzaneque, F., Morla, C., 2007. A palaeoecological interpretation of the lower–middle Pleistocene Cal Guardiola site (Terrassa, Barcelona, NE Spain) from the comparative study of wood and pollen samples. Rev. Palaeobot. Palynol. 146, 247–264. https://doi.org/10.1016/j.revpalbo.2007.05.003.

Pross, J., Koutsodendris, A., Christanis, K., Fischer, T., Fletcher, W.J., Hardiman, M., Kalaitzidis, S., Knipping, M., Kotthoff, U., Milner, A.M., Müller, U.C., Schmiedl, G., Siavalas, G., Tzedakis, P.C., Wulf, S., 2015. The 1.35-Ma-long terrestrial climate archive of Tenaghi Philippon, northeastern Greece: evolution, exploration, and perspectives for future research. nos 48, 253–276. https://doi.org/10.1127/nos/2015/0063.

Quézel, P., 1979. La région méditerranéenne française et ses essences forestières, signification écologique dans le contexte circum-méditerranéen. Forêt Méditerranéenne I, 7–18.

Quézel, P., Médail, F., 2003. Écologie et biogéographie des forêts du bassins méditerranéen. Elsevier. ed, Collection environnement, Paris.

Ravazzi, C., 1995. Paleobotany of the biogenic unit of the leffe formation (Early Pleistocene, northern Italy) : brief report on the state of ther art. IL Quaternario Italian. Journal of Quaternary Sciences 8, 435–442.

Ravazzi, C., Pini, R., Breda, M., Martinetto, E., Muttoni, G., Chiesa, S., Confortini, F., Egli, R., 2005. The lacustrine deposits of Fornaci di Ranica (late Early Pleistocene, Italian Pre-Alps): stratigraphy, palaeoenvironment and geological evolution. Quat. Int. 131, 35–58. https://doi.org/10.1016/j.quaint.2004.07.021.

Ravazzi, C., Rossignol Strick, M., 1995. Vegetation change in a climatic cycle of early pleistocene age in the leffe basin (northern Italy). Palaeogeogr. Palaeoclimatol. Palaeoecol. 117, 105–122. https://doi.org/10.1016/0031-0182(94)00118-R.

Ravazzi, C., Rossignol Strick, M., 1994. Interglacial-Glacial cycles in the early pleistocene of the Leffe Basin (Northern Italy) : preliminary report. Hist. Biol. 9, 11–15.

Reale, V., Monechi, S., 2005. Distribution of the calcareous nannofossil *Reticulofenestra asanoi* within the Early-Middle Pleistocene transition in the Mediterranean Sea and Atlantic Ocean: correlation with magneto- and oxygen isotope stratigraphy. SP (Sci. Prog.) 247, 117–130. https://doi.org/10.1144/GSL.SP.2005.247.01.06.

Reille, M., 1992. Pollen et spores d'Europe et d'Afrique du nord. Laboratoire de Botanique historique et Palynologie, Marseille.

Ricciardi, E., 1965. Analisi polliniche di una serie stratigrafica dei sedimenti lacustri del Pleistocene Inferiore nel Bacino di Leonessa (Rieti- Italia Centrale). G. Bot. Ital. 72, 62–82. https://doi.org/10.1080/11263506509430813.

Rivas-Martínez, S., 1981. Les étages bioclimatiques de la végétation de la péninsule ibérique. Anales del Jardin botanico de Madrid 37, 251–268.

Rohais, S., Joannin, S., Colin, J.-P., Suc, J.-P., Guillocheau, F., Eschard, R., 2007. Age and environmental evolution of the syn-rift fill of the southern coast of the gulf of Corinth (Akrata-Derveni region, Greece). Bull. Soc. Geol. Fr. 178, 231–243. https://doi.org/10.2113/gssgfbull.178.3.231.

Ruddiman, W.F., Raymo, M., McIntyre, A., 1986. Matuyama 41,000-year cycles: north Atlantic Ocean and northern hemisphere ice sheets. Earth Planet Sci. Lett. 80, 117–129. https://doi.org/10.1016/0012-821X(86)90024-5.

Saarinen, J., Oksanen, O., Žliobaitė, I., Fortelius, M., DeMiguel, D., Azanza, B., Bocherens, H., Luzón, C., Solano-García, J., Yravedra, J., Courtenay, L.A., Blain, H.-A., Sánchez-Bandera, C., Serrano-Ramos, A., Rodriguez-Alba, J.J., Viranta, S., Barsky, D., Tallavaara, M., Oms, O., Agustí, J., Ochando, J., Carrión, J.S., Jiménez-Arenas, J.M., 2021. Pliocene to Middle Pleistocene climate history in the Guadix-Baza Basin, and the environmental conditions of early Homo dispersal in Europe. Quat. Sci. Rev. 268, 107132. https://doi.org/10.1016/j.quascirev.2021.107132.

Sánchez Goñi, M.F., Llave, E., Oliveira, D., Naughton, F., Desprat, S., Ducassou, E., Hodell, D.A., Hernández-Molina, F.J., 2016a. Climate changes in south western Iberia and Mediterranean Outflow variations during two contrasting cycles of the last 1Myrs: MIS 31–MIS 30 and MIS 12–MIS 11. Global Planet. Change 136, 18–29. https://doi.org/10.1016/j.gloplacha.2015.11.006.

Sánchez Goñi, M.F., Rodrigues, T., Hodell, D.A., Polanco-Martínez, J.M., Alonso-García, M., Hernández-Almeida, I., Desprat, S., Ferretti, P., 2016b. Tropically-driven climate shifts in southwestern Europe during MIS 19, a low eccentricity interglacial. Earth Planet Sci. Lett. 448, 81–93. https://doi.org/10.1016/j.epsl.2016.05.018.

Sánchez-Garrido, J.C., Nadal, I., 2022a. The Alboran Sea circulation and its biological response: a review. Front. Mar. Sci. 9. https://doi.org/10.3389/fmars.2022.933390.

Sánchez-Garrido, J.C., Nadal, I., 2022b. The Alboran Sea circulation and its biological response: a review. Front. Mar. Sci. 9, 933390. https://doi.org/10.3389/fmars.2022.933390.

Sánchez-Laulhé, J.M., Jansa, A., Jiménez, C., 2021. Alboran Sea area climate and weather. In: Báez, J.C., Vásquez, J.-T., Camiñas, J.A., Malouli Idrissi, M. (Eds.), Alboran Sea - Ecosystems and Marine Resources, p. 939.

Sassoon, D., Lebreton, V., Combourieu-Nebout, N., Peyron, O., Moncel, M.-H., 2023. Palaeoenvironmental changes in the southwestern Mediterranean (ODP site 976, Alboran sea) during the MIS 12/11 transition and the MIS 11 interglacial and implications for hominin populations. Quat. Sci. Rev. 304, 108010. https://doi.org/10.1016/j.quascirev.2023.108010.

Sefidi, K., Marvie Mohadjer, M.R., Etemad, V., Copenheaver, C.A., 2011. Stand characteristics and distribution of a relict population of Persian ironwood (Parrotia persica C.A. Meyer) in northern Iran. Flora - Morphology, Distribution, Functional Ecology of Plants 206, 418–422. https://doi.org/10.1016/j.flora.2010.11.005.

Shackleton, N., Berger, A., Peltier, W.R., 1990. An alternative astronomical calibration of the lower Pleistocene timescale based on ODP Site 677, 81. Transactions of the Royal Society of Edinburgh : Earth Sciences, pp. 251–261.

Shaltout, M., Omstedt, A., 2014. Recent sea surface temperature trends and future scenarios for the Mediterranean Sea. Oceanologia 56, 411–443. https://doi.org/10.5697/oc.56-3.411.

Suc, J.-P., 1984. Origin and evolution of the Mediterranean vegetation and climate in Europe. Nature 307, 429–432. https://doi.org/10.1038/307429a0.
Suc, J.-P., Popescu, S.-M., 2005. Pollen records and climatic cycles in the North Mediterranean region since 2.7 Ma. SP (Sci. Prog.) 247, 147–158. https://doi.org/10.1144/GSL.SP.2005.247.01.08.
Suc, J.-P., Popescu, S.-M., Fauquette, S., Bessedik, M., Jiménez Moreno, G., Bachiri Taoufiq, N., Zheng, Z., Médail, F., Klotz, S., 2018. Reconstruction of Mediterranean flora, vegetation and climate for the last 23 million years based on an extensive pollen dataset. ecmed 44, 53–85. https://doi.org/10.3406/ecmed.2018.2044.
Suc, J.-P., Zagwijn, W.H., 1983. Plio-Pleistocene correlations between the northwestern Mediterranean region and northwestern Europe according to recent biostratigraphic and palaeoclimatic data. Boreas 12, 153–166. https://doi.org/10.1111/j.1502-3885.1983.tb00309.x.
Tintore, J., Violette, P.E.L., Blade, I., Cruzado, A., 1988. A study of an intense density front in the eastern Alboran Sea: the almeria–oran front. J. Phys. Oceanogr. 18, 1384–1397. https://doi.org/10.1175/1520-0485(1988)018<1384:ASOAID>2.0.CO, 2.
Toti, F., Bertini, A., Girone, A., Marino, M., Maiorano, P., Bassinot, F., Combourieu-Nebout, N., Nomade, S., Buccianti, A., 2020. Marine and terrestrial climate variability in the western Mediterranean Sea during marine isotope stages 20 and 19. Quat. Sci. Rev. 243, 106486. https://doi.org/10.1016/j.quascirev.2020.106486.
Tzedakis, P.C., Hooghiemstra, H., Pälike, H., 2006. The last 1.35 million years at Tenaghi Philippon: revised chronostratigraphy and long-term vegetation trends. Quat. Sci. Rev. 25, 3416–3430. https://doi.org/10.1016/j.quascirev.2006.09.002.
Van Der Wiel, A.M., Wijmstra, T.A., 1987a. Palynology of the 112.8–197.8 m interval of the core Tenaghi Philippon III, middle pleistocene of Macedonia. Rev. Palaeobot. Palynol. 52, 89–117. https://doi.org/10.1016/0034-6667(87)90048-0.
Van Der Wiel, A.M., Wijmstra, T.A., 1987b. Palynology of the lower part (78–120 M) of the core Tenaghi Philippon II, middle pleistocene of Macedonia, Greece. Rev. Palaeobot. Palynol. 52, 73–88. https://doi.org/10.1016/0034-6667(87)90047-9.
von Grafenstein, R., Zahn, R., Tiedemann, R., Murat, A., 1999. Planctonic δ18O records at sites 976 and 977, Alboran Sea: stratigraphy, forcing, and paleoceanographic implications. In: Proceedings of the Ocean Drilling Program. Scientific Results, pp. 469–479.
Wagner, B., Vogel, H., Francke, A., Friedrich, T., Donders, T., Lacey, J.H., Leng, M.J., Regattieri, E., Sadori, L., Wilke, T., Zanchetta, G., Albrecht, C., Bertini, A., Combourieu-Nebout, N., Cvetkoska, A., Giaccio, B., Grazhdani, A., Hauffe, T., Holtvoeth, J., Joannin, S., Jovanovska, E., Just, J., Kouli, K., Kousis, I., Koutsodendris, A., Krastel, S., Lagos, M., Leicher, N., Levkov, Z., Lindhorst, K., Masi, A., Melles, M., Mercuri, A.M., Nomade, S., Nowaczyk, N., Panagiotopoulos, K., Peyron, O., Reed, J.M., Sagnotti, L., Sinopoli, G., Stelbrink, B., Sulpizio, R., Timmermann, A., Tofilovska, S., Torri, P., Wagner-Cremer, F., Wonik, T., Zhang, X., 2019. Mediterranean winter rainfall in phase with African monsoons during the past 1.36 million years. Nature 573, 256–260. https://doi.org/10.1038/s41586-019-1529-0.
Wang, P., Tian, J., Lourens, L.J., 2010. Obscuring of long eccentricity cyclicity in Pleistocene oceanic carbon isotope records. Earth Planet Sci. Lett. 290, 319–330. https://doi.org/10.1016/j.epsl.2009.12.028.
Wang, Y., Li, C., Collinson, M.E., Lin, J., Sun, Q., 2003. *Eucommia* (Eucommiaceae), a potential biothermometer for the reconstruction of paleoenvironments. Am. J. Bot. 90, 1–7. https://doi.org/10.3732/ajb.90.1.1.
Zagwijn, W.H., 1974. The Pliocene-Pleistocene boundary in western and southern Europe. Boreas 3, 75–97. https://doi.org/10.1111/j.1502-3885.1974.tb00666.x.
Zhang, Z.-Y., Turland, N.J., 2003. Eucommiaceae. Flora of China 9.